The effect of ocean acidification on the carbon uptake behavior of the coccolithophore *Emiliania huxleyi*

Diplomarbeit

der Mathematisch-Naturwissenschaftlichen Fakultät
der Eberhard Karls Universität Tübingen

vorgelegt von

Dorothee Marie Kottmeier

Tübingen, November 2011

Erklärung:

Hiermit erkläre ich, dass ich diese Arbeit selbstständig verfasst und keine anderen als die angegebenen Quellen und Hilfsmittel benutzt habe.

Tübingen, den

Acknowledgements

I would like to thank everyone who contributed to this work. Special thanks go to:

Prof. Dr. Klaus Harter from ZMBP of the University of Tübingen for making my stay in Bremerhaven possible and for evaluating this thesis.

Prof. Dr. Dieter Wolf-Gladrow from the Marine Biogeochemistry Section of the Alfred-Wegener Institute for his support and for the evaluation of this thesis.

Dr. Björn Rost and Sebastian Rokitta of the ERC research group Phytochange for their excellent supervision, for sharing their knowledge with me, for their tremendous personal commitment and for being there for me at any time.

Laura Wischnewski and Ulrike and Klaus-Uwe Richter for the technical support.

All members of the Marine Biogeochemistry Section for their help and for keeping alive such a great atmosphere.

Mira Okshevsky and Rita Kottmeier for proof-reading this manuscript.

The members of the cooking group for the high-quality food and company.

Mar Fernandez and Erika Allhusen for making sure that I felt at home in Bremen right from the beginning.

My friends who are always there for me and who make my life so wonderful.

My sisters and parents for their love, their support, their motivation and their constant understanding.

List of contents

Zusammenfassung

In dieser Arbeit wurden die Auswirkungen der anthropogen verursachten Ozeanversauerung auf die Coccolithophoride *Emiliania huxleyi* untersucht. Hierzu wurden die Zellen des hochkalzifierenden Stammes RCC 1216 unter heutigen und unter in der Zukunft erwarteten CO_2-Partialdrücken (pCO_2; 380 and 950 μatm) angezogen. Um die ökophysiologischen Reaktionen auf unterschiedliche pCO_2-Werte zu ermitteln, wurden Wachstumsraten sowie Zellquotas und Produktionsraten von organischem und anorganischem Kohlenstoff gemessen. Mit Hilfe der ^{14}C-Disequilibrium-Methode wurden die relativen CO_2- und HCO_3^--Aufnahmeraten bestimmt. Diese Methode wird normalerweise bei einem relativ hohen pH-Wert von 8.5 durchgeführt, der häufig nicht dem pH-Wert in der Anzucht entspricht. Um einen möglichen Einfluss des pH-Wertes auf die relativen CO_2- und HCO_3^--Aufnahmeraten während der Messung abschätzen zu können, wurde die Methode abgewandelt und bei verschiedenen, ökologisch relevanten pH-Werten (pH 7.9, 8.1, 8.3, 8.5 und 8.7) durchgeführt. Die Robustheit der Methode wurde mittels einer Sensitivitätsstudie überprüft.

Erhöhte pCO_2-Werte führten zu gesteigerten Produktionsraten von organischem Kohlenstoff, während die Kalkbildung vermindert wurde. Die Wachstumsraten wurden nicht beeinflusst. Vergleichbare Reaktionen wurden auch in anderen Studien gezeigt. Die erweiterte ^{14}C-Disequilibrium-Methode konnte zeigen, dass die relativen CO_2- und HCO_3^- Aufnahmeraten stark von dem pH während der Messung beeinflusst werden. Bei niedrigem pH-Wert nahmen die Zellen bevorzugt CO_2 auf (pH 7.9 ≥90% CO_2-Nutzung), bei hohem pH-Wert wurde hingegen vor allem HCO_3^- aufgenommen (pH 8.7 ~25% CO_2-Nutzung). Im Gegensatz dazu hatten die Anzuchtsbedingungen keinen nennenswerten Einfluss auf das Aufnahmeverhalten. Die hier gezeigte vorherrschende CO_2-Nutzung bei typischen pH-Werten des Ozeans steht im Widerspruch zu anderen Studien, die eine überwiegende HCO_3^--Aufnahme für *E. huxleyi* postulieren. Die Sensitivitätsstudie bestätigte, dass die abgewandelte ^{14}C-Disequilibrium-Methode auch bei veränderten pH-Werten verlässliche Aussagen ermöglicht.

Die mit abnehmenden pH-Werten zunehmende relative CO_2-Nutzung könnte erklären, warum es bei erhöhtem pCO_2 zu gesteigerten Produktionsraten von organischem Kohlenstoff kommt. Durch die Erweiterung der ^{14}C-Disequilibrium-Methode konnten grundlegende Erkenntnisse über den Kohlenstofferwerb von *E. huxleyi* gewonnen werden, die in zukünftigen Prozessstudien zur Ozeanversauerung berücksichtigt werden sollten.

Summary

In this work, the effect of human-induced ocean acidification on the coccolithophore *Emiliania huxleyi* was examined. To this end, cells of the highly calcifying strain RCC 1216 were acclimated to present-day and expected future CO_2 partial pressures (pCO_2; 380 and 950 μatm). The ecophysiological responses were assessed by measuring growth rates as well as cellular quotas and production rates of organic and inorganic carbon. Applying the ^{14}C disequilibrium technique, the photosynthetic CO_2 and HCO_3^- uptake behavior of the differently treated cells was determined. This technique is usually carried out at the relatively high pH of 8.5, often being very different from acclimation pH. To assess possible effects of the assay pH on the carbon uptake behavior, the method was modified and applied over a range of ecologically relevant pH values (pH 7.9, 8.1, 8.3, 8.5 and 8.7). The reliability of the extended method was judged by performing model runs.

Elevated pCO_2 highly stimulated organic carbon production, but reduced the calcification of *E. huxleyi*. Growth rates, however, remained constant. While these results are in line with previous findings, the modification of the ^{14}C disequilibrium method provided new insights into modes of carbon acquisition. It was shown that the carbon uptake behavior of *E. huxleyi* strongly depends on the assay pH. At low pH, cells preferentially used CO_2 for carbon uptake (pH 7.9 ≥90% CO_2 usage), whereas at high pH primarily HCO_3^- was taken up (pH 8.7 ~25% CO_2 usage). In contrast, acclimation had no effect on the carbon uptake behavior. Hence, *E. huxleyi* mainly uses CO_2 as carbon source at typical pH values of the ocean, which contradicts previous assumption of predominant HCO_3^- usage. The sensitivity study indicated that the modified ^{14}C disequilibrium technique provides reliable results.

In conclusion, the higher biomass production at elevated pCO_2 could, in fact, be explained by the higher relative CO_2 usage determined under low pH. With this extension of the ^{14}C disequilibrium technique, new aspects about the mode of carbon acquisition were revealed, which should be considered for future process studies on ocean acidification effects.

List of abbreviations

C	Carbon
CA	Carbonic anhydrase
$CaCO_3$	Calcium carbonate
CCM	Carbon concentration mechanism
chl *a*	Chlorophyll *a*
C_i	Inorganic carbon
CO_2	Carbon dioxide
CO_3^{2-}	Carbonate ion
CRM	Certified Reference Material
DBS	Dextrane-bound sulfonamide
DIC	Dissolved inorganic carbon
eCA	External carbonic anhydrase
f_{CO2}	Fraction of CO_2 usage relative to net uptake
H^+	Proton
H_2CO_3	Carbonic acid
HCO_3^-	Bicarbonate
iCA	Internal carbonic anhydrase
K_m	Half-saturation (Michaelis) constant of enzyme/transporter
$K_{1/2}$	Half-saturation constant of process(es)
MIMS	Membrane-inlet mass spectrometry
N_2	Nitrogen
O_2	Oxygen
p	Pressure
pCO_2	Partial pressure of CO_2
PIC	Particular inorganic carbon
POC	Particular organic carbon
PON	Particular organic nitrogen
RubisCO	Ribulose-1,5-bisphosphate carboxylase/oxygenase
SA_{CO2}	Specific activity of CO_2
SA_{HCO3}	Specific activity of HCO_3^-
SA_{DIC}	Specific activity of DIC
S	Salinity
TA	Total alkalinity
T	Temperature
TPC	Total particular carbon
Ω	Carbonate saturation state of seawater
μ	Specific growth rate

List of figures & tables

1 Introduction

1.1 Phytoplankton and the global carbon cycle

Marine phytoplankton accounts for ~50% of global primary production (Falkowski et al. 1998) and strongly contributes to the vertical transport of carbon (C) from atmosphere and surface layers to the depths of the oceans. Beyond the build-up of particular organic carbon (POC), phytoplankton can influence the cycling of elements differently and is accordingly classified into functional groups (Rost et al. 2008). *Silicifiers*, mainly diatoms, play an important role in vertical fluxes of silicon by producing frustules made of biogenic silica. *Diazotrophs* (N_2-fixing cyanobacteria) contribute to marine productivity by increasing the concentration of bioavailable nitrogen. *Calcifiers*, mainly coccolithophores, are affecting marine biogeochemical cycling through production of particular inorganic carbon (PIC) in form of calcium carbonate ($CaCO_3$). Among the estimated ~5,000 marine phytoplankton species, only few contribute remarkably to the global elemental cycling (Falkowski and Raven 1997). One key calcifier is the very abundant and widespread coccolithophore *Emiliania huxleyi* that strongly contributes to the so-called *carbon pumps* (Sarmiento et al. 1995).

1.1.1 Biological carbon pumps

The ocean represents the largest carbon reservoir, which actively exchanges carbon dioxide (CO_2) with the atmosphere (on time scales of <10,000 years; Zeebe & Wolf-Gladrow 2007). The pool of dissolved inorganic carbon (DIC) is 50 times larger than the amount of CO_2 in the atmosphere (Falkowski et al. 2000). This can primarily be attributed to the fact that (in contrast to inert gases like oxygen (O_2) and nitrogen (N_2) CO_2 does not only dissolve but reacts with water to form ionic carbon species (see chapter 1.2). The vertical transport of DIC, governed by the carbon pumps, further enhances the overall storage capacity of the oceans.

The *solubility pump* describes the downward conveyance of cold, DIC-rich water at high latitudes, especially in the North Atlantic and in the Southern Ocean (CO_2 solubility increases with decreasing temperature). Reaching the ocean's interior, the deep-water masses are transported laterally until, up to several hundred years later, this water returns to the ocean's surface by upwelling, especially at continental shelves (Falkowski et al. 2000).

The biological pumps can be devided into the *organic carbon pump* and the *carbonate counter pump* (Fig. 1.1). The organic carbon pump is driven by the process of photosynthesis, fixing CO_2 into organic matter that is subsequently fed into the food web. Part of the organic matter sinks below the euphotic zone and reaches the ocean's interior, where its respiration and remineralization increase the concentration of DIC (Falkowski et al. 1998). Less than 1% of the former organic material ends up in sediments. The lowered DIC levels at the surface

promote the CO_2 resupply from the atmosphere and strongly contribute to the CO_2 uptake of the ocean.

The carbonate counter pump (Fig. 1.1) is driven by calcifying organisms and the subsequent sinking of $CaCO_3$, which at a certain depth starts to dissolve. As the precipitation of $CaCO_3$ reduces the DIC concentration and total alkalinity (TA; see chapter 1.2) in a molar ratio of 1:2, the relatively stronger decrease in TA causes a shift in chemical equilibrium towards higher CO_2 concentrations. Somewhat counter-intuitively, this process can therefore act as a CO_2 source for the atmosphere (Zeebe & Wolf-Gladrow 2007).

Relative strength of the two biological carbon pumps is represented by the *rain ratio*, which determines the CO_2 fluxes between surface water and atmosphere. Both pumps are inter-dependent, however, which is best illustrated by the example of coccolithophores, producing $CaCO_3$ as well as organic matter. $CaCO_3$ can act as ballast material for organic matter aggregates, accelerating their sinking rate and therefore increasing the transfer efficiency to depth (Armstrong et al. 2002; Klaas & Archer 2002).

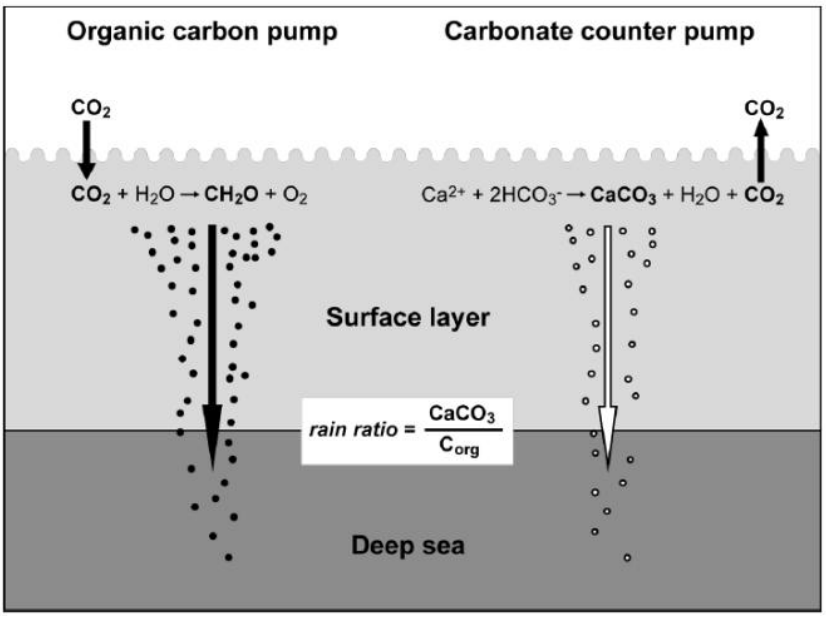

Fig. 1.1: The biological carbon pumps. The *organic carbon pump* induces a CO_2 in-gassing at the surface of the ocean, whereas the carbonate counter pump can cause CO_2 out-gassing. Relative strength of both pumps is reflected in the *rain ratio* (graph: Rost and Riebesell, 2004).

1.1.2 Climate change

For the last ~850,000 years, atmospheric partial pressures of CO_2 (pCO_2) have fluctuated between 180 and 300 μatm (1 atm = $1.0133 \cdot 10^5$ Pa) in glacial and interglacial times, respectively (Fig. 1.2; Petit et al. 1999; Lüthi et al. 2008). Anthropogenic perturbations, however, have caused the pCO_2 to increase in an unprecedented rate to values, higher than those recorded for the last 20 million years (Pearson & Palmer 2000). Since pre-industrial times, pCO_2 increased from 280 μatm to presently 385 μatm and is expected to reach 750 μatm by the end of this century (IPCC Scenario IS92a; Pacala et al. 2001). Other scenarios even predict values of ≥1000 μatm for the year 2100 (Raupach et al. 2007; Solomon et al. 2007).

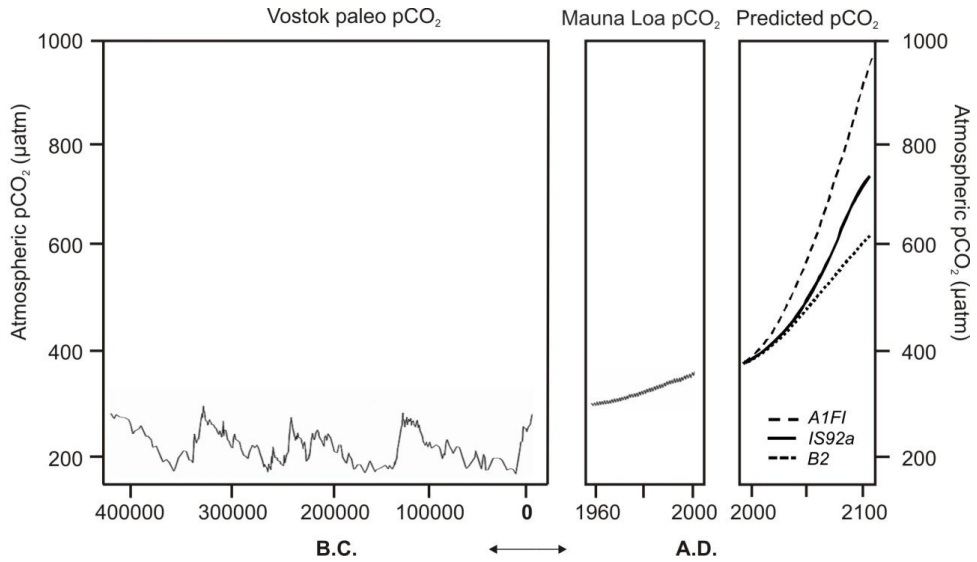

Fig. 1.2: Changes in pCO_2 recorded in ice cores (Vostok core; Petit et al. 1999), directly measured (Mauna Loa; http://www.esrl.noaa.gov/gmd/ccgg/trends) and predicted in a 'sustainability' scenario (*B2*), a 'business-as-usual' scenario (*IS92a*), and a 'worst-case' scenario (*A1FI*; Solomon et al. 2007).

Increasing pCO_2 will directly affect the marine carbonate system by elevating the concentration of DIC, altering carbon speciation and lowering the pH of the seawater (*ocean acidification*). As a greenhouse gas, elevated pCO_2 causes global warming (2 to 6°C until the year 2100, IPCC 2007). The higher temperatures of the surface ocean, in turn, will lead to stronger stratification and shallower mixing of the water column. Stratification willdiminish the nutrient supply to the upper mixed layer, where mean light intensities increase (Rost & Riebesell 2004; Sarmiento et al. 2004). These direct and indirect CO_2 effects are expected to impact phytoplankton in many ways, which may feedback on the biological pumps and therefore climate.

Some physiological processes like photosynthesis or calcification were found to be especially sensitive to changes in carbonate chemistry. In order to understand the effects of global change on phytoplankton, a thorough understanding of the marine carbonate system and the underlying physiological processes is crucial. To begin with the chemical aspects, a short introduction into the carbonate system is given below.

1.2 The Marine carbonate system

1.2.1 Basics of the carbonate system

The surface of the ocean constantly exchanges CO_2 with the atmosphere. The equilibration is described by Henry's law:

$$[CO_2]_{(aq)} = K_0 \cdot pCO_2 \quad (1)$$

where K_0 is the temperature (T) and salinity (S) dependent solubility constant of CO_2 in seawater (Weiss 1974). $CO_{2(aq)}$ reacts with water (H_2O) to carbonic acid (H_2CO_3), which successively dissociates to bicarbonate (HCO_3^-) and carbonate ions (CO_3^{2-}), releasing protons (H^+; Fig. 1.3). Since the concentration of H_2CO_3 is negligible (<0.3 % of DIC, Stumm & Morgan 1996), its concentration is typically included in the $[CO_2]$.

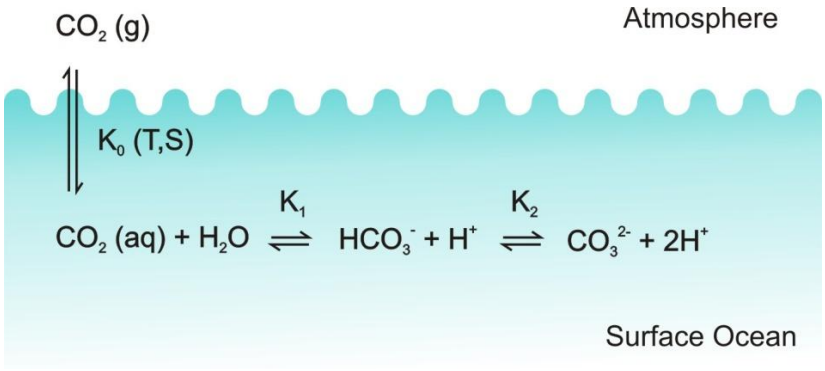

Fig. 1.3: Scheme of the marine carbonate system. Fluxes of CO_2 (g) and CO_2 (aq) are determined by *Henry's law*. The equilibrium constants K_1 and K_2 describe the relative proportion of the different carbon species (graphics T. Eberlein).

The equilibration between the carbon species can be described by the stoichiometric equilibrium constants (K_1^* and K_2^*) of the law of mass action, which depend on S, T and pressure (p):

$$K_1^* = \frac{[HCO_3^-][H^+]}{[CO_2]} \quad (2)$$

$$K_2^* = \frac{[CO_3^{2-}][H^+]}{[HCO_3^-]} \quad (3)$$

The hydration of CO_2 is a relatively slow process compared to the interconversion of HCO_3^- and CO_3^{2-}. The kinetics of the reaction between CO_2 and HCO_3^- can be described with the rate constants k_+ and k_-:

$$K_1^* = \frac{[HCO_3^-][H^+]}{[CO_2]} = \frac{k_+}{k_-} \quad (4)$$

Rate constants reflect the rate at which equilibrium is restored after a disequilibrium has been induced. The constants k_+ and k_- are dependent on S, T and p and pH value.

The relative abundance of the carbon species is dependent on TA, [DIC], S, p and T. All parameters show a complex interdependence. Two parameters of the carbonate system are of special interest as they are not dependent on T and p. One of them is DIC, the sum of the dissolved inorganic carbon species:

$$DIC = [CO_2] + [HCO_3^-] + [CO_3^{2-}] \tag{5}$$

The other conservative parameter is TA, a property of the ocean that is closely related to the buffer capacity of seawater. TA has been defined as the excess of H^+ acceptors over H^+ donors with respect to zero level of H^+ (Dickson 1981; Zeebe & Wolf-Gladrow 2007):

$$\begin{aligned} TA = {} & [HCO_3^-] + 2[CO_3^{2-}] + [B(OH)_4^-] + [OH^-] \\ & + [HPO_4^{2-}] + 2[PO_4^{3-}] + [H_3SiO_4^-] \\ & + [NH_3] + [HS^-] - [H^+]_F - [HSO_4^-] - [HF] - [H_3PO_4] \end{aligned} \tag{6}$$

with $[H^+]_F$ being the free concentration of hydrogen ions. At seawater pH >8, mainly carbonate ($[HCO_3^-]$ + $[CO_3^{2-}]$), borate ($[B(OH)_4^-]$) and water alkalinity ($[OH^-]$ - $[H^+]$) contribute to TA. TA can also be defined as the total concentrations of certain major ions (Na^+, Cl^-, Ca^{2+} etc.) and the total concentrations of various acid-base species (total phosphate etc.; Wolf-Gladrow et al. 2007). This definition includes parameters that are not affected by changes in p and T, hence being referred to as the explicit conservative definition of TA:

$$\begin{aligned} TA_{EC} = {} & [Na^+] + 2[Mg^{2+}] + 2[Ca^{2+}] + 2[Sr^{2+}] \\ & + \ldots - [Cl^-] - [Br^-] - [NO_3^-] \ldots - (T)PO_4 \\ & + TNH_3 - 2TSO_4 - THF - THNO_2 \end{aligned} \tag{7}$$

with $(T)PO_4 = [H_3PO_4] + [H_2PO_4^-] + [HPO_4^{2-}] + [PO_4^{3-}]$, $TNH_3 = [NH_3] + [NH_4^+]$, $TSO_4 = [SO_4^{2-}] + [HSO_4^-]$, $THF = [F^-] + [HF]$, and $THNO_2 = [NO_2^-] + [HNO_2]$ being the total phosphate, ammonia, sulphate, fluoride and nitrite, respectively (Wolf-Gladrow et al. 2007).

Knowing two of the six variables [CO_2], [HCO_3^-], [CO_3^{2-}], [H^+], DIC and TA, all other parameters can be calculated (Zeebe & Wolf-Gladrow 2007). The DIC speciation can be illustrated in the Bjerrum plot (Fig. 1.4). At present pH of the ocean, 90% of the DIC species is available as HCO_3^-, 9% as CO_3^{2-} and only small fractions exist in form of CO_2 (<1%; with S = 34, p = 1 atm, T = 25°C).

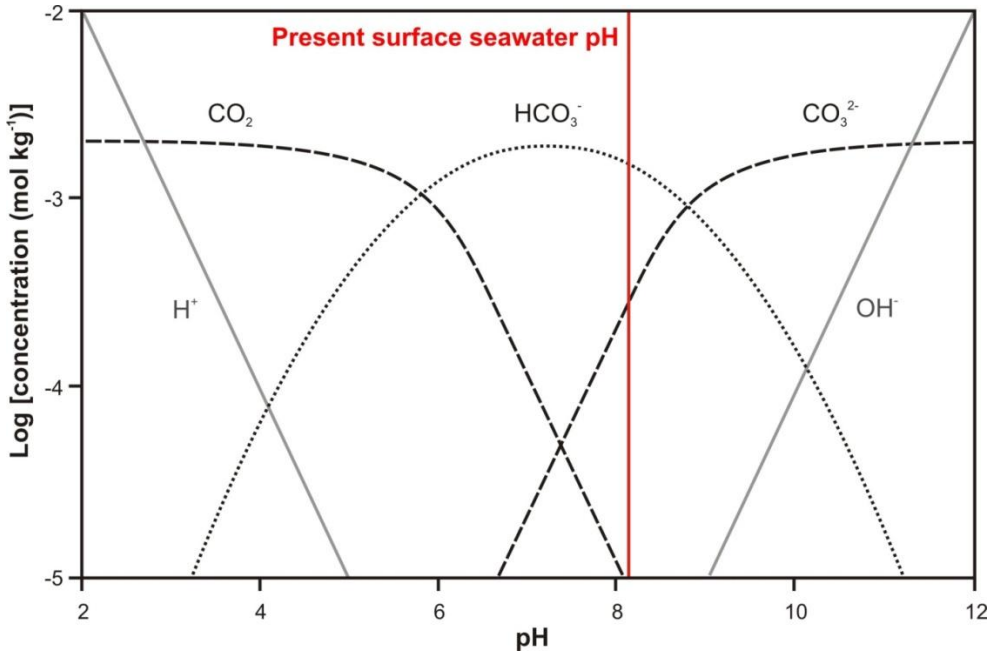

Fig. 1.4: Carbon speciation of seawater, presented in a Bjerrum plot. The concentrations of the different inorganic carbon species CO_2, HCO_3^- and CO_3^{2-} are determining the pH of the seawater and vice versa. Today's surface seawater pH, based on present day's pCO_2 of 380 μatm, a salinity of 34 and a temperature of 25°C is indicated by the vertical line (graphics T. Eberlein).

1.2.2 Effect of biological processes

Biological processes can influence the carbonate chemistry in different ways (Fig. 1.5). Through the process of organic matter production, [DIC] decreases and TA slightly increases due to the co-occurring nitrate uptake. The reverse reaction of organic matter remineralization increases [DIC] and decreases TA correspondingly. The process of calcification reduces DIC and TA in a 1:2 ratio, because in the reaction:

$$Ca^{2+} + CO_3^{2-} \rightarrow CaCO_3 \tag{8}$$

one molecule of CO_3^{2-} is consumed, that counts twice in TA, but only once in DIC. $CaCO_3$ dissolution increases DIC and TA in the same ratio.

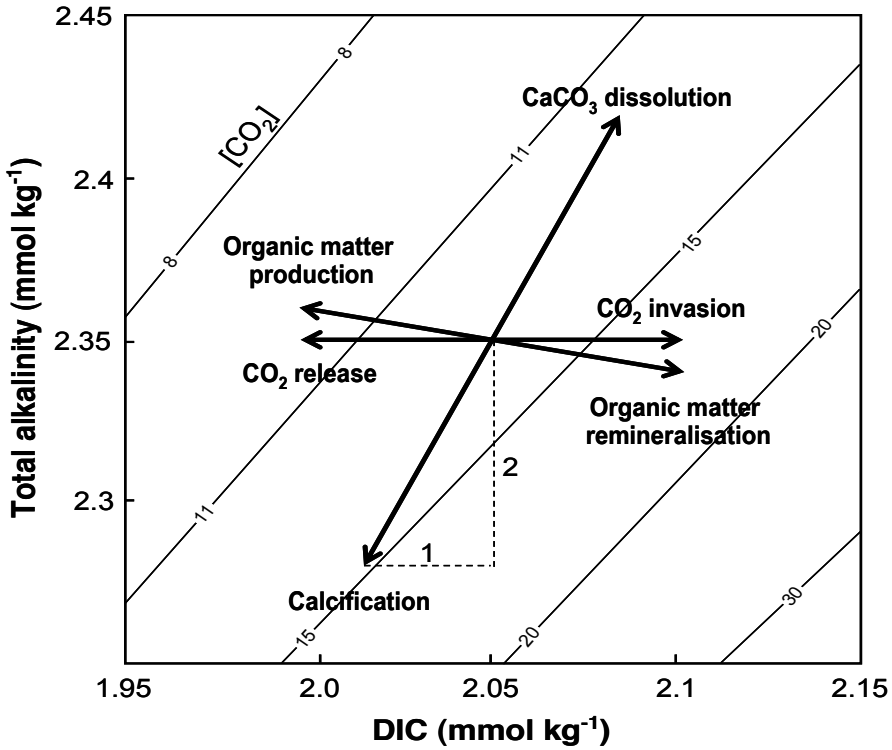

Fig. 1.5: Effect of biological processes on carbonate chemistry. Lines indicate levels of dissolved CO_2 in μmol kg^{-1} as a function of DIC and TA (modified after Zeebe & Wolf-Gladrow 2007).

1.2.3 Effect of rising atmospheric pCO_2

With increasing atmospheric pCO_2 the ocean takes up more DIC (*carbonation*), altering carbon speciation and lowering the pH of the seawater (*acidification*). When pCO_2 rises from 280 to 750 µatm, for instance, CO_2 concentration triples, HCO_3^- concentration increases by ~10 %, and CO_3^{2-} concentration decreases by ~40%, leading to a decrease of pH by 0.4 units (Fig. 1.6). The shift in the carbonate system can influence physiology of phytoplankton. To estimate possible effects of elevated pCO_2 on cell physiology, especially on the modes of carbon uptake, the underlying mechanisms are described in the following in more details.

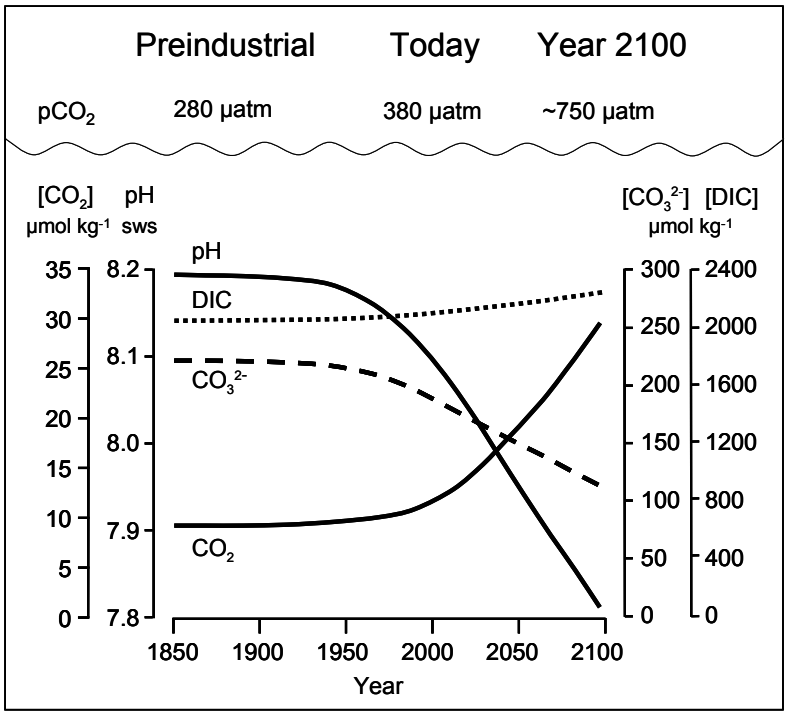

Fig. 1.6: Predicted changes of the carbonate chemistry referring to the IPCC IS92a scenario (modified after Zeebe & Wolf-Gladrow 2007).

1.3 Carbon acquisition mechanisms

The demand for inorganic carbon (C_i) in phytoplankton cells is mainly attributed to their photosynthetic carbon assimilation. The process of photosynthesis consists of two different pathways: In the light reaction, energy is captured to drive the production of ATP and NADPH. In the dark reaction, CO_2 or O_2 are substrates for the enzyme Ribulose-1,5-bisphosphate carboxylase/ oxygenase (RubisCO). While the carboxylating reaction is the entry point of CO_2 into the Calvin-Benson cycle and serves the generation of energy-rich molecules, the oxygenase reaction initiates the energy dissipative photorespiration (Asada 1999).

In coccolithophores, the other C_i demanding process is calcification. The $CaCO_3$ precipitation takes place in intracellular coccolith vesicles. The underlying mechanism is, however, not completely understood (Taylor & Brownlee 2005) and the carbon source is still unknown. For a long time photosynthesis was suspected to rely on "CO_2 delivery" by calcification (Sikes & Wilbur 1980). In the meantime, it has been demonstrated that the C_i fluxes associated with photosynthesis are independent from Ci fluxes for calcification (Riebesell et al. 2000; Rost et al. 2002; Herfort et al. 2004; Trimborn et al. 2007).

1.3.1 Carbon concentration mechanisms

RubisCO is an ancient enzyme that evolved in times of high CO_2 and low O_2 concentration. As the affinity for CO_2 is very low, the competition between CO_2 and O_2 is high under present day conditions. Under present CO_2 concentration in seawater (≤10 to ~30 μmol kg^{-1}, Reinfelder 2011), RubisCO is at or below half-saturation constants of RubisCO (K_m, 20 to 185 μmol L^{-1}). The slow CO_2 diffusion in water as well as the slow conversion between CO_2 and HCO_3^- cause CO_2 concentrations to be even lower in the cell's boundary layer. This explains why the enzyme is very susceptible to carbon limitation under today's pCO_2 (Badger et al. 1998). As a consequence, various types of *carbon concentration mechanisms* (CCMs) have evolved in many phytoplankton species to increase the CO_2 concentration in the vicinity of RubisCO (Raven 1997; Badger et al. 1998). Also calcification could rely on modes of CCMs, but there is still little knowledge because most research focused on the role of CCMs in photosynthesis.

Presence of CCM is indicated when i) rates of photosynthesis exceed the rates expected from diffusive CO_2 supply only, ii) C_i affinity of the cell is higher than the C_i affinity of RubisCO and iii) a higher internal than external CO_2 or DIC concentration is observed (Badger et al. 1998; Reinfelder 2011). CCMs include active uptake of CO_2 and/or HCO_3^- by specific transporters as well as a variety of external and/or internal carbonic anhydrases (CAs). These enzymes catalyze the conversion between CO_2 and HCO_3^- and has been found in all phytoplankton taxa, but so far their role in CCMs is still not always understood (Trimborn et al. 2008). Efficient C_i accumulation is only achieved, when C_i uptake is

combined with processes to minimize the loss of C_i. This can be realized by certain properties of plasma membrane, pyrenoid structure or by localized C_i accumulation in the chloroplast. For some diatom species, also the C4-like pathway has been proposed to be a component of the CCM (Reinfelder et al. 2000; Reinfelder 2004), but so far this pathway has only been identified for one species (Tortell et al. 2006; Roberts et al. 2007; Trimborn et al. 2008).

Species relying on diffusive CO_2 uptake or those with inefficient CCMs are thought to be very sensitive to increased CO_2 availability and are likely to benefit from higher CO_2 concentrations. Even species being close to CO_2 saturation, but being able to regulate their CCM, might have advantages from higher pCO_2 by optimized energy and resource allocation (Rost et al. 2008), for instance, by downregulation of the CCM activity (Kranz et al. 2010). Marine diatoms and the haptophyte genus *Phaeocystis* are considered to have high efficient CCMs (e.g. Tortell et al. 2002; Rost et al. 2003; Trimborn et al. 2009). Coccolithophores are assumed to have low efficient CCMs, e.g. represented in high $K_{1/2}$ of CO_2 or DIC dependent O_2 evolution in comparison to other taxa (e.g. Rost et al. 2003).

1.3.2 Methodology in research on carbon uptake

First studies on C_i acquisition made use of kinetic approaches to determine C_i affinities of cells and the O_2/CO_2 sensitivity of C_i fixation (Graham and Whittingham 1968; Berry et al. 1976). Later on, studies using silicone oil centrifugation verified the existence of intracellular accumulation of C_i and the ability of cells to transport HCO_3^- over the cell membrane (Badger et al. 1977, 1980; Kaplan et al. 1980). More recent work, using membrane-inlet mass spectrometry (MIMS), made major advances towards understanding the CO_2 and HCO_3^- fluxes (Badger et al. 1994; Sültemeyer et al. 1995). Many conclusions about the relative usage of CO_2 and HCO_3^- have been drawn from the ^{14}C disequilibrium technique (Espie & Colman 1986; Elzenga 2000), which proved well suitable for field studies (Tortell & Morel 2002; Cassar et al. 2004; Martin & Tortell 2006; Tortell et al. 2008; Tortell et al. 2010).

The ^{14}C disequilibrium technique is based on the relatively slow conversion between HCO_3^- and CO_2 in seawater (Johnson 1982), allowing differential labeling of the two C_i species. A transient isotopic disequilibrium is induced by adding a small volume of an "acidic" $DI^{14}C$ sike solution (pH 7.0; ~ 20% of DIC is CO_2) to a large volume of alkaline cell suspension (pH 8.5; ~0.4% of DIC is CO_2). As a consequence, the specific activity of CO_2 (SA_{CO2}, [dpm mol^{-1}]) is initially high and decays exponentially to an equilibrium value. Specific activity of HCO_3^- (SA_{HCO3}) stays more or less constant during the assay (Fig. 1.7a).

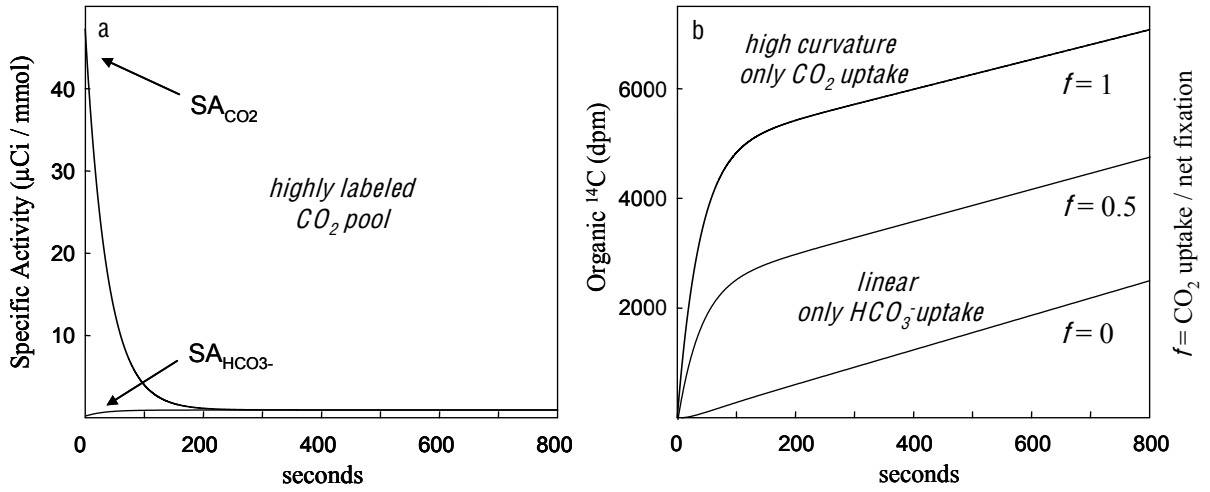

Fig. 1.7: ^{14}C disequilibrium technique: (a) Theoretical time-course of specific activities of CO_2 and HCO_3^- after spiking and (b) theoretical ^{14}C incorporation curves.

Upon spike addition, cells incorporate the ^{14}C into biomass and the corresponding accumulation of radioactivity is monitored over time (Fig. 1.7b). Depending on which C_i species the cells use as carbon source, the initial slope of the incorporation curve differs. Cells only taking up HCO_3^- show linear ^{14}C incorporation, while cells using CO_2 only, initially show a steep increase in ^{14}C incorporation that levels off when the isotopic equilibrium is achieved. An intermediate curvature in ^{14}C incorporation indicates a mixture of CO_2 and HCO_3^- uptake. The fraction of CO_2 usage relative to net C_i uptake (f_{CO2}) can be derived from fitting the measured ^{14}C incorporation with the adequate mathematical equation (see Material and methods).

This method is a very reliable approach to unravel relative C_i usage, but it relies on certain assumptions. First of all, the photosynthetic rate of the cells has to stay constant during the assay. Second, possible eCA activity has to be prevented to assure the slow kinetics of the conversion between CO_2 and HCO_3^- (otherwise equilibrium would be achieved too fast). Third, pH during the assay does not directly influence the C_i uptake behavior. While the first assumptions are typically controlled, the influence of the relatively high pH of 8.5 on C_i acquisition has never been tested. For this reason, this study investigated the effect of the assay pH on the relative CO_2/HCO_3^- usage in the coccolithophore *E. huxleyi*.

Emiliania huxleyi – an important coccolithophore

Emiliania huxleyi is the most abundant and wide-spread coccolithophore, and a well-known bloom-forming species. Because of its special biogeochemical role, it has been in the focus of research for a long time (Westbroek et al. 1993). Blooms can cover over 10,000 km^2 (Merico et al. 2003), being very dense (≤10,000 cells mL^{-1} and ≤300,000 free coccoliths mL^{-1}). Remote sensing of blooms is possible due to the light scattering properties of the calcite shells (coccoliths) that are shed from the cells (Holligan et al. 1993).

Calcification of *E. huxleyi* seems to suffer from ocean acidification, while photosynthesis was often shown to be stimulated (Paasche 1964; Nielsen 1995; Riebesell et al. 2000; Berry et al. 2002; Zondervan et al. 2002; Leonardos & Geider 2005; Langer et al. 2009; Hoppe et al. 2011). Also natural communities dominated by *E. huxleyi* were sensitive to elevated pCO_2 (Engel et al. 2005; Riebesell et al. 2007; Schulz et al. 2007). Langer (2006, 2009) pointed out, that physiological responses to elevated pCO_2 are varying not only between species but also between strains. The sensitivity is also dependant on light and nutrient availability (e.g. Zondervan 2007; Rokitta & Rost subm.).

E. huxleyi have been shown to take up primarily HCO_3^- (Rost et al. 2006; Trimborn et al. 2007; Rokitta & Rost subm.). This active mode of C_i uptake was also indicated by molecular approaches (von Dassow et al. 2009; Rokitta et al. 2011; Rokitta & Rost subm.). Furthermore, there are indications for active CO_2 transport in this species (e.g. Schulz et al. 2007). In contrast to diatoms and *Phaeocystis*, no or very low eCA activities have been detected in *E. huxleyi* so far (Elzenga et al. 2000; Rost et al. 2003), but there is physiological and molecular evidence for iCAs being present in the species (e.g. Rost et al. 2003; von Dassow et al. 2009; Richier et al. 2011). It has been suspected that the mode of C_i acquisition of *E. huxleyi* is causal for the exceptional sensitivity towards ocean acidification (Raven & Johnston 1991; Rost et al. 2008).

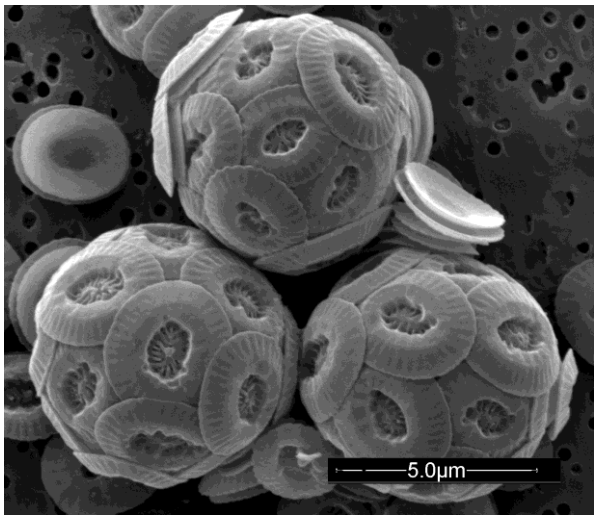

Fig. 1.8: Scanning electron microscope images of *E. huxleyi* strain RCC 1216 (photo C. Hoppe).

1.4 Aim of the study

The aim of this thesis was to get new insights into the C_i acquisition of *E. huxleyi* and its sensitivity towards ocean acidification. To this end, cells were acclimated to different pCO_2 levels of 380 and 950 µatm to i) measure responses in growth and elemental composition and ii) assess the carbon uptake behavior under these conditions. To compare the instantaneous effects during the assay with the acclimation effects, a modified version of the *standard disequilibrium technique* was applied at several ecologically relevant pH values (pH 7.9, 8.1, 8.3, 8.5 and 8.7). The ^{14}C incorporation under equilibrium was used to estimate the pH-dependence of total C_i fixation rates. The reliability of the new technique was tested by performing model runs.

2 Material and methods

2.1 Growths conditions

Diploid cells of the highly calcifying *E. huxleyi* strain RCC 1216 (obtained from the Roscoff culture collection) were grown at 15°C as semi-continuous cultures at a 16:8 h light:dark cycle in North Sea seawater under acclimation pCO_2 of 380 and 950 μatm. The seawater medium was sterile-filtered (0.2 μm) and enriched with vitamins and trace metals (Table 2.1, Guillard & Ryther, 1962). Phosphate and nitrate were added in concentrations of 100 and 6.25 μmol L^{-1}, reflecting the Redfield N:P ratio of 16:1 (Redfield, 1963).

Table 2.1: Components and concentrations of the seawater medium (Guillard & Ryther, 1962)

	substance	[μmol L^{-1}]
nutrients:	NaNO3	100
	HNa_2PO_4	6.25
metals:	$MnSO_4 * H_20$	0.915
	$ZnSO_4 * 7 H_20$	0.0765
	$CoSO_4 * 7 H_20$	0.0425
	$CuSO_4 * 5 H_20$	0.0395
	$Na_2MoO_4 * 2 H_20$	0.026
	$Na_2EDTA * 2H_2O$	11.65
	$FeCl_3 * 6 H_20$	1.94
		[g L^{-1}]
vitamins:	cyanocobalamin	0.001
	biotin	0.001
	thiamin * HCl	0.2

The media were aerated for at least 36 h with humidified, 0.2 μm-filtered air with a pCO_2 of 380 or 950 μatm before usage. The according gas mixtures were created by a gas flow controller (CGM 2000 MCZ Umwelttechnik, Bad Nauheim, Germany) using pure CO_2 (Air Liquide Deutschland, Düsseldorf, Germany) and CO_2-free air (CO2RP280, Dominick Hunter, Willich, Germany). The pCO_2 was controlled regularly with a non-dispersive infrared analyzer system (LI6252, LI-COR Biosciences, Bad Homburg, Germany), which was calibrated with CO_2-free air and purchased gas mixtures of 150 ±10 and 1000 ±20 μatm CO_2 (Air Liquide, Düsseldorf, Germany). The gas flow rate was adjusted to 130 ±10 mL min^{-1}. Culturing was carried out in 2.4 L sterilized borosilicate bottles (Duran Group, Mainz, Germany) on a roller table to avoid sedimentation of cells. The light was provided by Biolux 19W/965 daylight lamps (OSRAM, Munich, Germany), where the photon flux density was adjusted to ~300 μmol photons m^{-2} s^{-1} with a datalogger LI-1400 (LI-COR, Lincoln, NE, USA) using a 4π-sensor (US-SQS/L, Walz, Effeltrich, Germany).

2.2 Carbonate chemistry

The carbonate system was controlled by measuring pH, DIC and TA in the acclimation. The pH_{NBS} of the acclimations was measured potentiometrically and corrected for temperature (pH meter 3110; WTW, Weilheim, Germany with a SenTix 41 electrode). The electrode was two-point calibrated with NBS certified standard buffers (pH 9.180 ±0.02, WTW, Weilheim, Germany and pH 6.865 ±0.015, Mettler-Toledo, Urdorf, Switzerland).

The DIC samples were filtered through syringe-filters (cellulose acetate, 0.2 μm, Thermo Fisher Scientific, Rochester, NY, USA) into 5 mL borosilicate bottles with PTFE septum and stored at 8°C. DIC was determined colorimetrically according to Stoll et al. (2001) using a TRAACS CS800 autoanalyzer (Seal Analytical, Norderstedt, Germany). For the analysis, samples were acidified with sulphuric acid (H_2SO_4) to a pH <1 to convert all C_i species into CO_2, subsequently being transferred to an absorbing indicator substance via a silicon membrane. The amount of CO_2 was determined by measuring the change of extinction at a wavelength of 550 nm.

The TA of the samples was determined by potentiometric titration with an automated burette system (TitroLine alpha plus, Schott Instruments, Mainz, Germany). Samples of 25 mL were titrated with 0.05 M HCl (S = 35) and the resulting pH was monitored. TA was calculated from linear Gran-titration plots (Dickson 1981), plotting the added volume of acid versus proton concentration. DIC and TA samples were accuracy-corrected with Certified Reference Materials (CRMs, Batch No. 111) supplied by A. Dickson (Scripps Institution of Oceanography, USA).

The carbonate system (Table 2.2) was calculated from pH_{NBS} and TA, temperature (T = 15 °C) and salinity (S = 32.4) using CO_2sys, running on Excel (Pierrot et al. 2006). For all calculations, phosphate and silicate concentrations were assumed to be 10.3 μmol kg^{-1} and 7.4 μmol kg^{-1}, respectively, based on colorimetric measurements of media with a continuous flow analyzer (Evolution III, Alliance Instruments, Salzburg, Austria). Equilibrium constants for carbonic acid, K_1 and K_2 given by Mehrbach et al. (1973), refit by Dickson & Millero (1987) were used. For the dissociation of sulphuric acid, constants assessed by Dickson (1990) were applied.

Table 2.2: Measured and calculated parameters of the carbonate system at the end of the acclimation experiments.

	measured:			*calculated:*			
acclimation	TA [μmol kg^{-1}]	DIC [μmol kg^{-1}]	pH_{NBS} at 15 °C	pCO_2 [μatm]	CO_2 [μmol kg^{-1}]	HCO_3^- [μmol kg^{-1}]	CO_3^{2-} [μmol kg^{-1}]
380 μatm	2276 ±1	2045 ±3	8.170 ±0.011	351 ±9	13 ±0	1,863 ±9	163 ±3
950 μatm	2285 ±13	2161 ±9	7.826 ±0.033	891 ±38	33 ±3	2,080 ±28	83 ±6

2.3 Ecophysiological response

The response of the cells to the respective acclimation was derived from growth as well as their elemental compositions. The examined parameters were POC, PIC, total particular carbon (TPC) and particular organic nitrogen (PON). In addition, chlorophyll *a* (chl *a*) was determined. Growth was monitored by daily cell counting with a Multisizer III hemocytometer (Beckman-Coulter, Fullerton, CA, USA). The specific growth rate μ was calculated from:

$$\mu = \frac{(\ln c_2 - \ln c_1)}{t_2 - t_1} \tag{9}$$

with t_1 and t_2 [d] being the time points of sampling and c_1 and c_2 being the cell concentrations at t_1 and t_2, respectively.

Cell harvesting took place four to eight hours after the beginning of the light period (i.e. at midday) at densities of 40,000 to 60,000 cells mL^{-1} (in exponential growth). Acclimations that showed a pH drift >0.05 units compared to a cell-free reference medium were excluded from further analysis. Cells were pre-acclimated to the respective conditions for at least 7 days, i.e more than 10 divisions.

For the measuring of the elemental composition, defined volumes of cell suspension were filtered with vacuum pumps (suction pressure of -200 mbar) onto pre-combusted (12h, 500°C) GF/F filters (1.2 μm; Whatman, Maidstone, UK). For the quantification of POC, the PIC fraction was removed by acidifying the filters with 200 μL 0.2 M HCl. After drying, the non-acidified as well as the acidified filters were wrapped with carbon-free tin foil to be subsequently analyzed for the N/C content with an ANCA-SL 20-20 mass spectrometer (SerCon Ltd., Crewe, UK). ANCA measurements are based on a flash oxidation of the samples, converting all C and N containing components to CO_2 and NO_X (subsequently reduced to N_2). These gases were then quantified by the mass spectrometer. Measurements were corrected with blank filters.

Quotas for TPC, POC and PON could be directly deduced from the respective filters, considering cell densities and volume filtered. Quotas for PIC were calculated by substracting POC from TPC quotas. By multiplying TPC, POC and PIC quotas with specific growth rates, the respective production rates were derived.

For chl *a* measurements, cells were filtered onto cellulose nitrate filters (Sartorius, Göttingen, Germany), which were stored in darkness at -20°C until measurement. Chl *a* was extracted in 90% acetone (Sigma, Munich, Germany) and determined fluorometrically (TD-700 fluorometer, Turner Designs, Sunnyvale, USA) following the protocol by Holm-Hansen & Riemann (1978). The calibration of the fluorometer was carried out with a commercially available standard (*Anacystis nidulans*, Sigma, Steinheim, Germany). From the determined chl *a* contents of the samples, the chl *a* quota and chl *a*:POC ratios were determined.

2.4 Bioassay

2.4.1 Carbon source assessment

To determine the preferential carbon source of photosynthesis, the *^{14}C disequilibrium technique* was applied. As an extension to the conventional assay at pH 8.5, the method was carried out over a range of ecologically relevant pH values (7.9, 8.1, 8.3, 8.5 and 8.7). Correspondingly, the pH of the ^{14}C spike had to be adjusted to get a similar magnitude in the initial isotopic disequilibrium ($\Delta SA_{CO2}/SA_{DIC}$; Table 2.3). Buffer chemicals for assay media and spike solutions were chosen to work optimally at given pH values (Good et al. 1966). Assay buffers were prepared up to 3 weeks in advance and stored in gas tight containers to keep DIC concentration constant. The used seawater batch had a [DIC] of ~2250 μmol kg^{-1} and a salinity of 32.4. To verify the assumption that neither pH nor DIC drifted significantly over time, values were controlled prior to the measurements.

Table 2.3: Carbonate system, buffers and fitting parameters used for the modified ^{14}C disequilibrium technique

medium pH_{NBS}	*medium buffer*	$\frac{CO_2}{DIC_{medium}}$	*spike pH_{NBS}*	*spike buffer*	$\frac{CO_2}{DIC_{spike}}$	$CO_{2\,medium}$ [µmol kg^{-1}]	$\alpha 1$	$\alpha 2$	$\frac{\Delta SA_{HCO3-}}{SA_{DIC}}$	$\frac{\Delta SA_{CO2}}{SA_{DIC}}$
7.9	BICINE	1.45%	5.75	MES	81.08%	32.5	0.0176	0.0183	-0.808	55.0
8.1	BICINE	0.90%	6.35	MES	51.84%	20.2	0.0194	0.0206	-0.514	56.6
8.3	BICINE	0.55%	6.70	MES	32.46%	12.4	0.0223	0.0246	-0.321	58.0
8.5	BICINE	0.33%	7.00	HEPES	19.41%	7.4	0.027	0.0312	-0.191	57.7
8.7	BICINE	0.19%	7.30	HEPES	10.77%	4.3	0.0344	0.043	-0.106	54.7

The experiments were carried out four to eight hours after the beginning of the light period. Prior to ^{14}C spike addition, acclimated cells were concentrated to about $2{,}5 \cdot 10^6$ cells mL^{-1} by gentle filtration on a polycarbonate filter (2 μm, Millipore, Billerica, MA, USA). During this procedure, in which cells were always kept in suspension and growth temperature (T = 15°C), the assay medium was gradually exchanged with 50 mM BICINE buffered seawater medium of the appropriate pH. Four milliliter of that cell suspension were transferred into a temperature controlled (15°C) cuvette. To eliminate any possible CA activity, 10 μL of 50 μM dextrane-bound sulfonamide (DBS; Ramidus, Lund, Sweden) was added. The cells were continuously stirred and illuminated at 300 μmol photons m^{-2} s^{-1} at least six minutes prior spike addition.

Spike solutions were prepared by adding 10 µL of $NaH^{14}CO_3$ solution (2.15 GBq/mmol, GE Healthcare, Amersham, UK) into 190 µL of correspondingly buffered (50 mM) deionized water (Table 2.3). After spike addition, 200 µL subsamples were taken at 5, 10, 15, 20, 30, 60, 120, 240, 340, 440, 540 and 640 seconds and transferred into 2 mL 6 M HCl, instantaneously inducing cell death and converting PIC to DIC. DI^{14}C was driven out of the samples by shaking them for several days before 10 mL of scintillation cocktail (Ultima Gold AB, Packard) were added. Incorporated radioactivity was counted with a Packard Tri-Carb Liquid

scintillation counter (GMI, Ramsey, MN, USA). For each assay run, 2 to 3 blank samples, consisting of cell-free medium being adequately spiked with ^{14}C, were treated alongside the other samples.

To determine the relative CO_2 usage, data were fitted according to equations derived from Espie & Colman (1986) and Elzenga et al. (2000). The instantaneous rate of ^{14}C incorporation is the sum of $^{14}CO_2$ and $H^{14}CO_3^-$ uptake at any given time:

$$d(dpm_t)/dt = V_{CO_2} \times SA_{CO_2 t} + V_{HCO_3^-} \times SA_{HCO_3^- t} \quad (10)$$

with $d(dpm_t)/dt$ being the instantaneous rate of ^{14}C uptake at time t and V_{CO2} and V_{HCO3-} being the uptake rates for CO_2 and HCO_3^-, respectively. $SA_{CO2,t}$ and $SA_{HCO3,t}$ are the time-dependent specific activities of CO_2 and HCO_3^-, respectively. Following Martin & Tortell (2006), the f_{CO2} value was determined by fitting the integrated ^{14}C incorporation:

$$\begin{aligned} dpm = {} & V_t(f)(\alpha_1 t + (\Delta SA_{CO_2}/SA_{DIC})(1-e^{-\alpha 1 t}))/\alpha_1 \\ & + V_t(1-f)(\alpha_2 t + (\Delta SA_{HCO_3}/SA_{DIC})(1-e^{-\alpha 2 t}))/\alpha_2 \end{aligned} \quad (11)$$

with V_t being the total rate of ^{14}C incorporation, SA_{DIC} being the specific activity of the DIC. ΔSA is the change of the specific activity between the initial and equilibrium value of CO_2 and HCO_3^-, respectively, and α_1 and α_2 are the pH-, temperature-, and salinity-dependent rate constants calculated according to Espie & Colman (1986). Since the assay was performed over a range of pH values, the variable parameters in the fitting equation ($\alpha 1$, $\alpha 2$, $\Delta SA_{HCO3-}/SA_{DIC}$, $\Delta SACO_2/SA_{DIC}$) were adjusted to the conditions of the spike and buffer solutions (pH, S, T) modifying equilibrium constants of Johnson (1982) and Millero & Roy (1997). The respective parameters are given in Table 3.1.

From final slopes of ^{14}C incorporation curves, also C_i fixation rates were calculated and normalized to chl *a*:

$$C_i\,fix = V_{equ} \cdot SA_{DIC}^{-1} \cdot 1.05 \cdot chl\ a^{-1} \quad (12)$$

with $C_i fix$ being the C_i fixation rate, V_{equ} being the rate of ^{14}C uptake (d(dpm)/dt) in equilibrium and 1.05 reflects the fractionation factor (Vogel et al. 1970).

2.4.2 Sensitivity study

To assess the sensitivity to erroneously assays conditions, ideal data was fit using parameters ($\alpha 1$, $\alpha 2$, $\Delta SA_{HCO3}/SA_{DIC}$, $\Delta SA_{CO2}/SA_{DIC}$) based on diverged pH (±0.05 units) and T (±2°C). These scenarios were tested under low pH (7.90) and high pH (8.70) for a high CO_2 usage (f_{CO2} = 0.80) and low CO_2 usage (f_{CO2} = 0.25). The results for f_{CO2} estimates were then compared with the ideal data, e.g. the correct f_{CO2} value of the given condition.

To evaluate the influence of error afflicted blanks on f_{CO2} estimates, the fit was applied to data for which blanks were over and underestimated (±100 dpm). The effect of blank

correction was tested under scenarios of low and high pH, high and low CO_2 usage, as well as different final ^{14}C incorporation rates (1, 2, 4 and 8 dpm per sec).

2.5 Statistics

Experiments were performed in at least biological triplicates. Acclimation data was statistically evaluated by performing Student´s t-tests. Physiology data was analyzed with one way ANOVAs and subsequent Multiple comparison tests that were based on t-tests comparing the datasets pair wise. Null hypotheses (i.e. data is significantly different) were rejected when $p \leq 0.05$. Statistical significance was divided in three significance levels with * indicating $p \leq 0.05$, ** indicating $p \leq 0.01$ and *** indicating $p \leq 0.001$.

3 Results

3.1 Ecophysiological response

Specific growth rates (μ) of cells acclimated to low pCO_2 (380 μatm) did not differ significantly from those of cells acclimated to elevated pCO_2 (950 μatm; Fig. 3.1). The mean μ of both acclimations was 1.06 ±0.05 d^{-1} (corresponds to ~1.5 divisions d^{-1}).

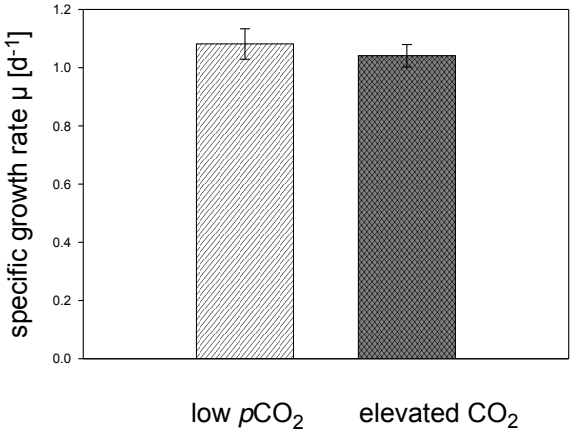

Fig. 3.1: Specific growth rates in response to acclimation at low (~380 µatm) and elevated (~950 µatm) pCO_2. Error bars indicate 1 SD, n ≥3.

The acclimation at elevated pCO_2 caused a significant increase of the POC quota from ~8 to 15 pg $cell^{-1}$ (+87%; Fig. 3.2a). Consequently, the POC production rate was also significantly increased from ~9 to 15 pg $cell^{-1}$ d^{-1} (+81%; Fig. 3.2b). The PIC quota, in contrast, was insignificantly decreased from ~12 to 11 pg $cell^{-1}$ (Fig. 3.2c) and the PIC production significantly decreased from ~13 to 11 pg $cell^{-1}$ d^{-1} in response to elevated pCO_2 (Fig. 3.2d). Being the sum of PIC and POC, the TPC quota and TPC production showed a smaller increase than POC. The TPC quota increased by 27% from ~20 to 25 pg $cell^{-1}$ (Fig. 3.2e), while the production of TPC increased by 22% from ~22 to 27 pg $cell^{-1}$ d^{-1} (Fig. 3.2f).

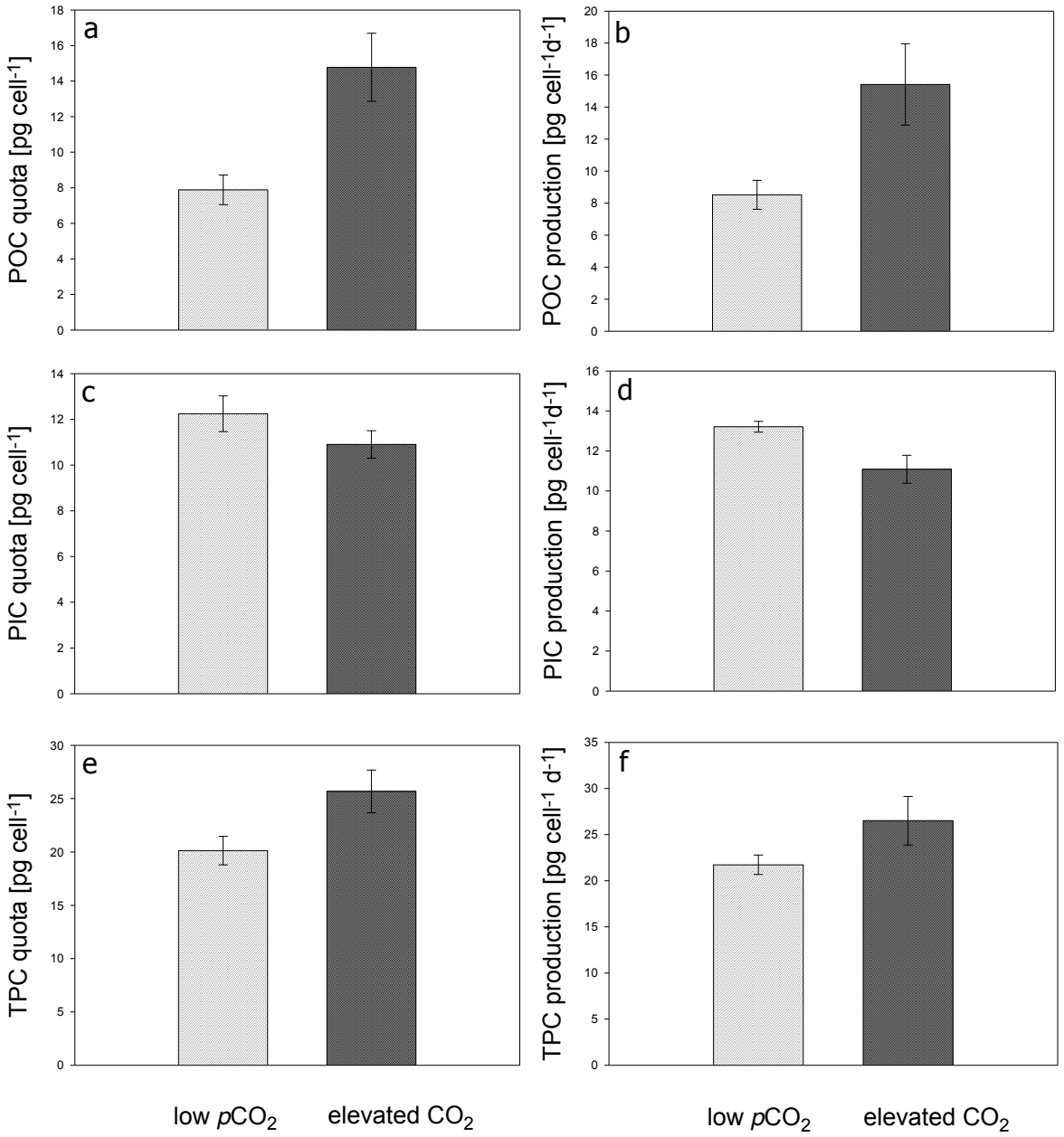

Fig. 3.2: Ecophysiological response to acclimation at low (~380 μatm) and elevated (~950 μatm) pCO_2. (a) POC quota, (b) POC production, (c) PIC quota, (d) PIC production, (e) TPC quota, (f) TPC production. Error bars indicate 1 SD, n ≥3.

At elevated pCO_2, owing to the distinct response pattern in PIC versus POC, molar PIC:POC ratio strongly changed from ~1.6 to 0.8 (Fig. 3.3a). The molar POC:PON ratio increased significantly from ~6.6 to 8.8 (Fig. 3.3b). Chl *a* quota increased from ~0.11 to 0.17 (Fig. 3.3c). After normalization to POC, however, the Chl *a*:POC ratio was unaltered by elevated pCO_2 (0.013 ±0.0022 pg pg^{-1}; Fig. 3.3d).

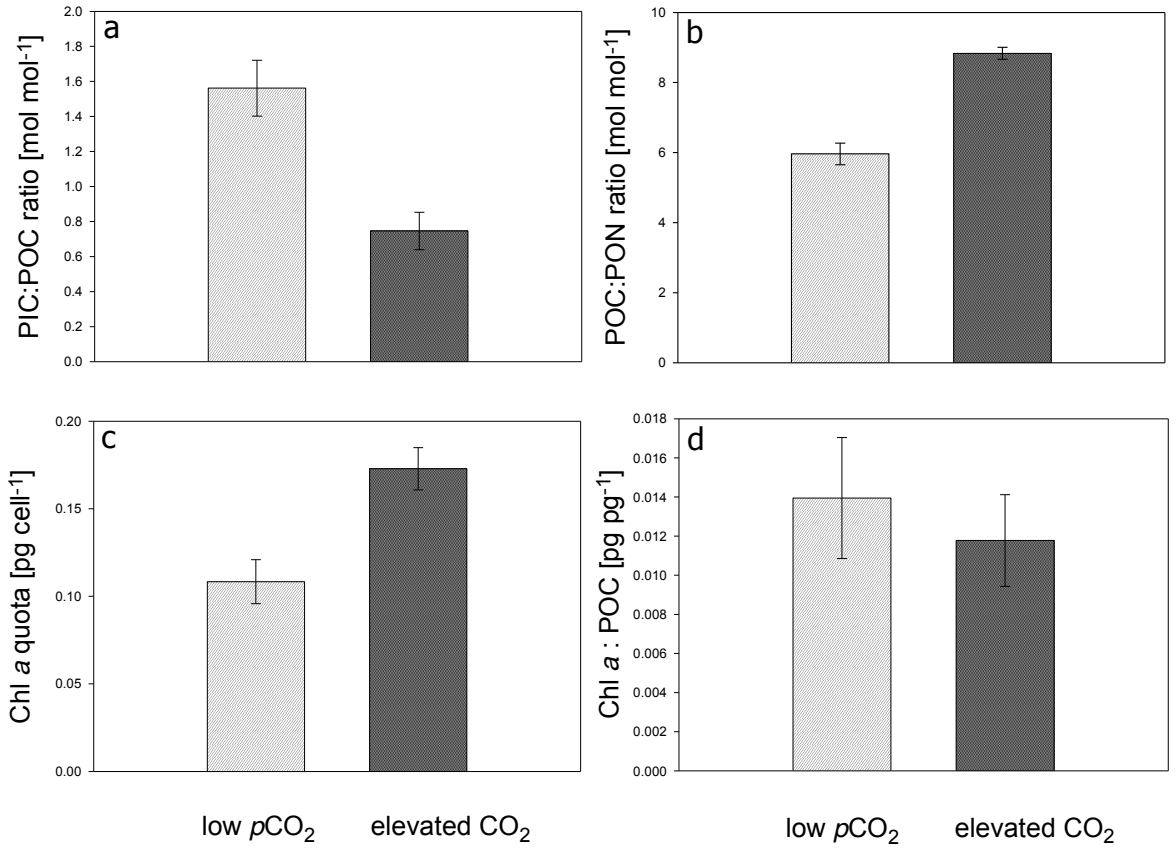

Fig. 3.3: Ecophysiological response to acclimation at low (~380 µatm) and elevated (~950 µatm) pCO_2. (a) Molar PIC:POC ratio, (b) molar POC:PON ratio, (c) chl *a* quota, (d) chl *a*:POC. Error bars indicate 1 SD, n ≥3.

3.1 Bioassay

3.2.1 Carbon source assessment

The ^{14}C disequilibrium technique was performed over a range of ecologically relevant pH values for cells, acclimated to low (~380 μatm) and elevated (~950 µatm). In Figure 3.4, examples for ^{14}C incorporation curves of 'CO_2 users' and 'HCO_3^- users' are shown.

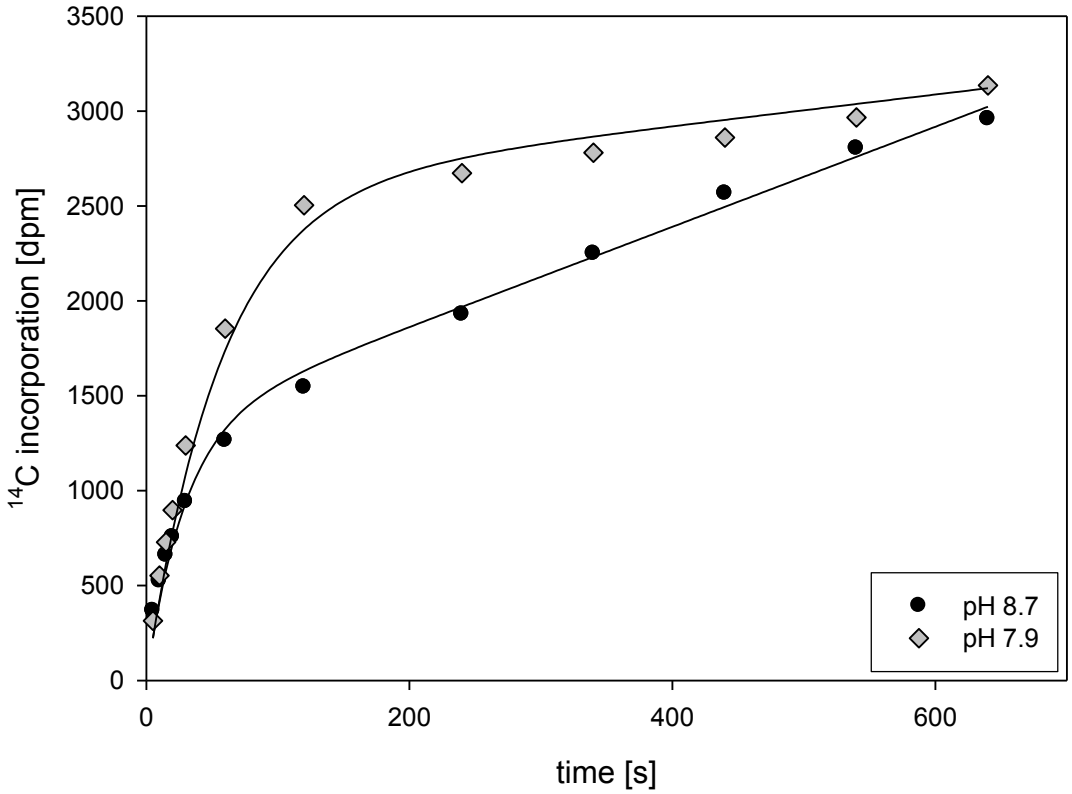

Fig. 3.4: Exemplary ^{14}C incorporation curves. At pH 7.9 (grey diamonds) *E.huxleyi* preferentially used CO_2 as carbon source (here f_{CO2} = 1.00); hence their ^{14}C incorporation over time shows a steep curvature. At pH 8.7 (black circles), cells preferentially used HCO_3^- as carbon source (here f_{CO2} = 0.32); hence the curvature of the ^{14}C incorporation curve was less steep. Continuous lines indicate the fitted curves. Please note that cells were from the same incubation (pCO_2 380 μatm).

The instantaneous pH during the measurements altered the relative CO_2 usage f_{CO2} (Fig. 3.5). With increasing pH in the assay medium, cells progressively changed their preference from CO_2 (>90% CO_2 usage at pH 7.9) to HCO_3^- (~75% HCO_3^- usage at pH 8.7). While pH affected the relative CO_2 usage, only small differences between the acclimations were observed. At elevated pCO_2, f_{CO2} seemed to decrease slightly for all assay pH values. This effect was however insignificant.

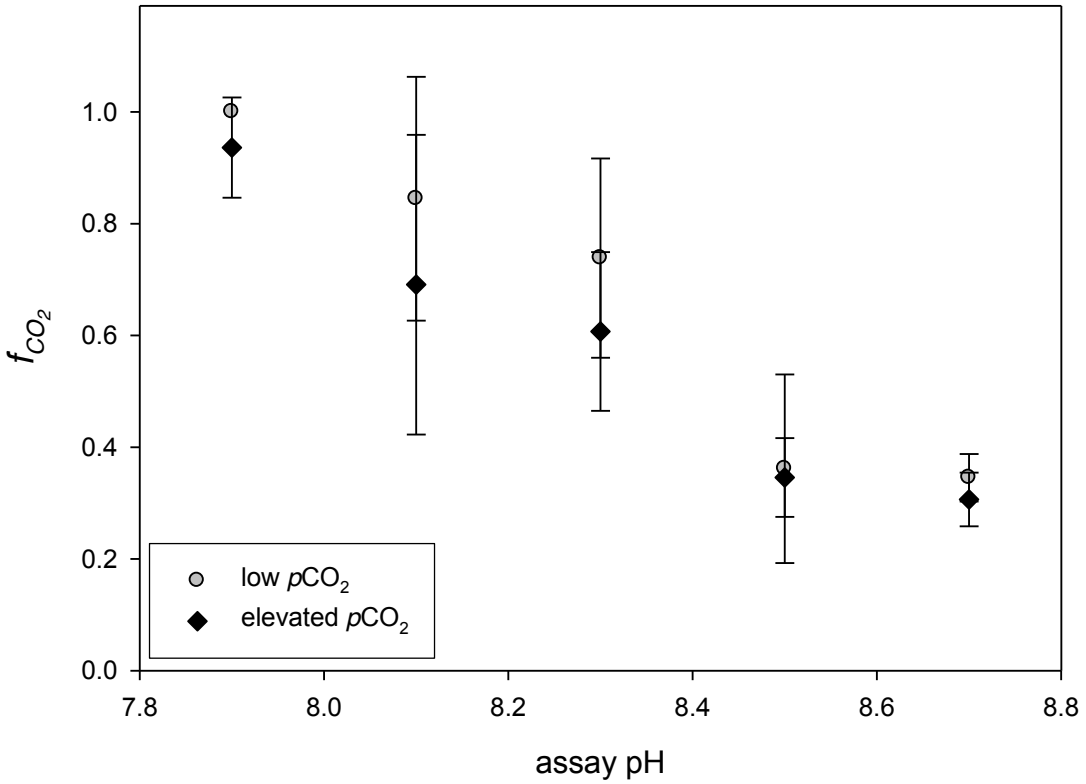

Fig. 3.5: Relative CO_2 usage (f_{CO2}) as a function of assay pH for cells acclimated to low pCO_2 (~380 μatm; grey circles) and elevated pCO_2 (~950 μatm; black diamonds). Error bars indicate 1 SD, n ≥3. Corresponding statistical significance is presented in Table 3.2.

Measured pH values and DIC concentration of the used assay media at time of assay performance are shown in Table 3.1 pH drift corrected fitting yielded similar f_{CO2} values as using the initial pH values (results not shown), but these adjustments increased the level of significance in some cases (Table 3.2).

Table 3.1: Measured pH of assay medium and spike as well as DIC concentration of assay medium and resulting CO_2 concentrations and adjusted fitting parameters (α1, α2, $\Delta SA_{HCO3}/SA_{DIC}$, $\Delta SA_{CO2}/SA_{DIC}$).

Medium pH	Spike pH	[DIC] [µmol kg^{-1}]	[CO_2] [µmol kg^{-1}]	[CO_2] [µmol kg^{-1}]	α_1	α_2	$\frac{\Delta SA_{HCO3-}}{SA_{DIC}}$
7.904	5.807	2158	30.82	0.0177	0.0184	-0.7868	54.0
8.098	6.401	2204	19.91	0.0194	0.0206	-0.4843	53.1
8.288	6.761	2237	12.69	0.0221	0.0243	-0.2906	51.0
8.516	7.043	2328	7.38	0.0275	0.0320	-0.1748	55.0
8.704	7.277	2097	4.01	0.0346	0.0433	-0.1112	58.0

Table 3.2: Statistical analysis of the pH-dependent carbon uptake behavior, with * indicating p ≤0.05, ** p ≤0.01 and *** p ≤0.001. Asterisks in brackets represent significances that only occur when ^{14}C incorporation curves were fit with equations adapted to measured assay pH.

	Assay pH	pH 8.7	pH 8.5	pH 8.3	pH 8.1	pH 7.9
380 µatm	pH 8.7			(*)	**	***
	pH 8.5			*	**	***
	pH 8.3	(*)	*			
	pH 8.1		**			
	pH 7.9	***	***			
1000 µatm	pH 8.7					**
	pH 8.5					(*)
	pH 8.3					
	pH 8.1					
	pH 7.9	**	(*)			-

3.2.2 Sensitivity study

In the sensitivity study, the consequences for f_{CO2} estimation due to errors in the pH, T and blank measurements were determined (Fig. 3.6). Incorrect estimation of the assay pH had a stronger effect on determined f_{CO2} values in cells with high CO_2 usage (errors ≤20 percentage points) than on cells with high HCO_3^- usage (errors ~6 percentage points). Also offsets in spike pH had a bigger impact on CO_2 users (errors ≤20 percentage points) than on HCO_3^- users (errors ≤6 percentage points). Offsets in assay temperature influenced mainly f_{CO2} estimates of CO_2 users (≤20 percentage points) and less HCO_3^- users (≤4 percentage points).

Modeling the consequences of incorrect blank estimates indicated that absolute errors in f_{CO2} estimates are decreasing with increasing ^{14}C uptake rates (Fig. 3.7). Errors in f_{CO2} estimates were ≤20 percentages points and ≤5 percentage points when DI^{14}C uptake rate were ≥4 and 8 dpm s^{-1} respectively. Absolute errors in blank estimates affected f_{CO2} values of CO_2 users slightly more.

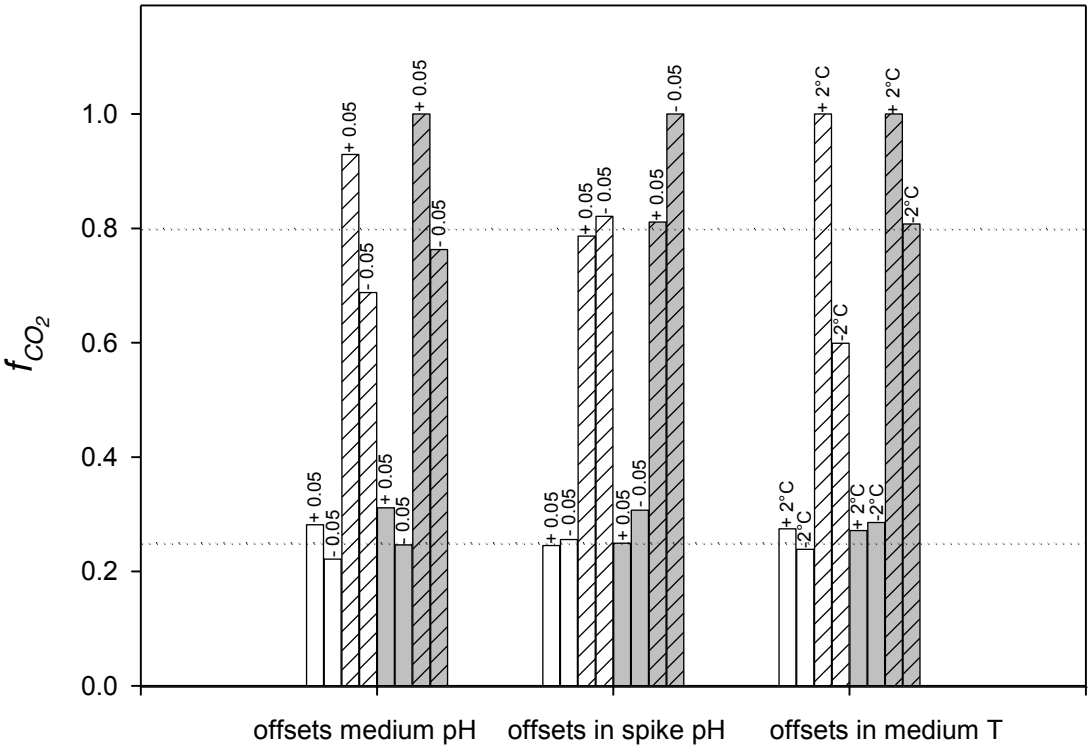

Fig. 3.6: Sensitivity of f_{CO2} estimates in response to errors in pH and temperature. Tested offsets were ±0.05 pH units and ±2°C, respectively. The symbols + and – indicate a positive and negative offset in pH or T, respectively. The white bars represent assay conditions of pH 7.9, grey bars assay conditions of pH 8.7.

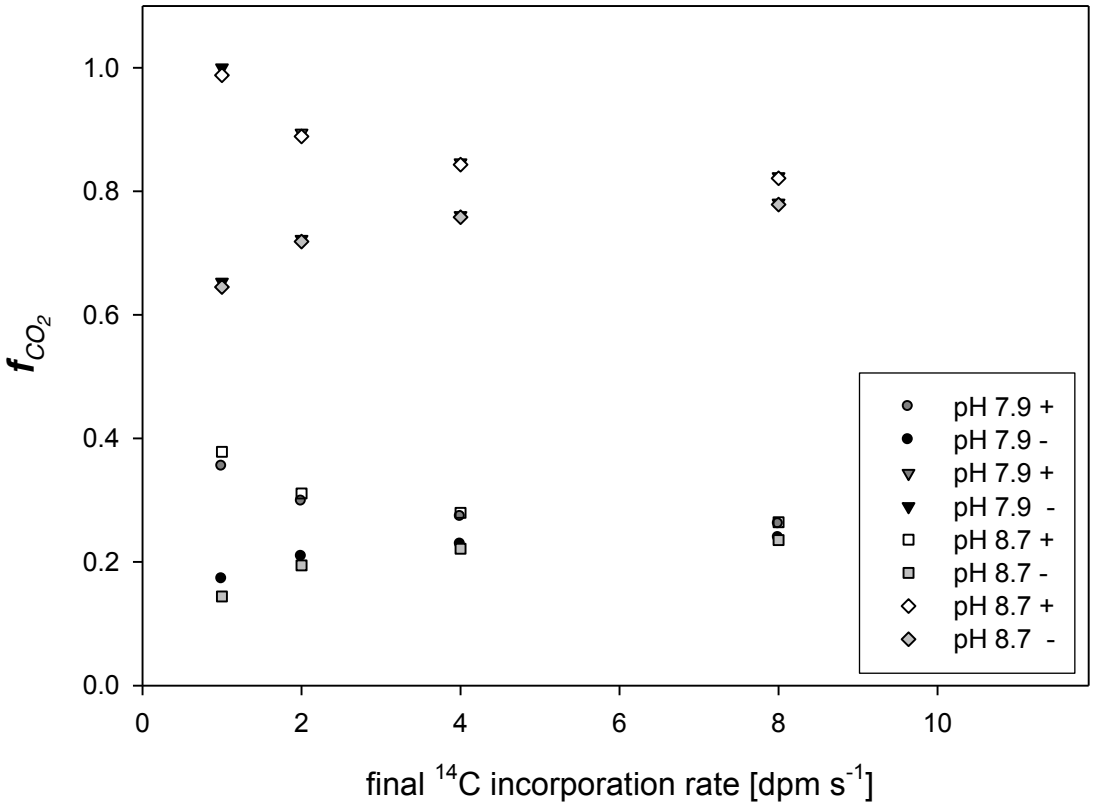

Fig. 3.7: Sensitivity of f_{CO2} estimates in response to errors in blank measurements. The symbol + and – indicate a positive and a negative blank offset of 100dmp, respectively. The pH values given in the legend describe the assay conditions for which the consequences of offsets were tested.

3.2.3 Carbon fixation rates

C_i fixation rates obtained from final slopes of ^{14}C incorporation curves were between ~30 and 250 µmol (mg chl *a*$^{-1}$) h^{-1} and did not alter significantly with changing assay pH values (Fig 3.8). Differences between acclimation and pH during the assay could not be detected, possibly due to the high variability between the replicates.

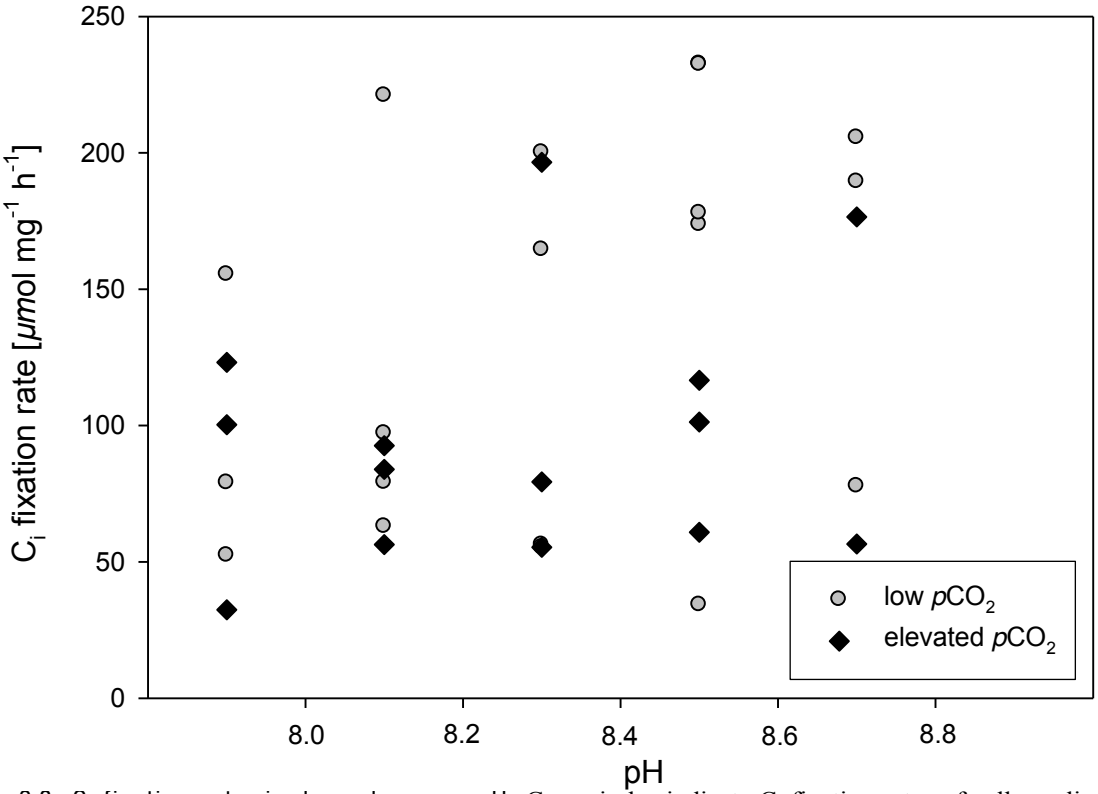

Fig. 3.8: C_i fixation rates in dependence on pH. Grey circles indicate C_i fixation rates of cells acclimated to low pCO_2 (~380 µatm), black diamonds indicate rates of cells acclimated to elevated pCO_2 (~950 µatm).

4 Discussion

The sensitivity of *E. huxleyi* strain RCC 1216 to ocean acidification was investigated by measuring the ecophysiological response to acclimations under different pCO_2 (380 and 950 μatm). In addition, possible pH-dependent regulation of the cellular carbon uptake behavior was assessed. Responses in growth and elemental composition are in line with previous findings. With the extension of the ^{14}C disequilibrium technique, new aspects regarding the mode of C_i acquisition were revealed, which should be considered for future process studies on ocean acidification effects.

4.1 Ecophysiological response

While growth rates were not affected by elevated pCO_2, quotas and production rates of POC strongly increased. However, the quotas and production of PIC decreased (Fig. 3.2). These findings are generally in line with several other studies that were performed with *E. huxleyi* (e.g. Riebesell et al. 2000; Berry et al. 2002; Langer et al. 2006, 2009; Hoppe et al. 2011) and even with the very same strain (Rokitta & Rost subm.). The stimulation of POC production indicates that net C_i fixation benefits from elevated pCO_2, which in principle can be attributed to altered respiration and/or C_i acquisition. While there is only little evidence for lowered respiration rates under elevated pCO_2 (Raghavendra & Padmasree 2003), modes of C_i acquisition have often been held responsible for CO_2/pH effects on POC production. The latter aspect will be discussed in chapter 4.2.

In contrast to the beneficial effect on biomass production, PIC production seems to suffer from ocean acidification. Langer & Bode (2011) assumed that lowered PIC production is directly caused by higher CO_2 concentration, while Suffrian et al. (2011) argued that calcification is less efficient due to the higher internal H^+ concentration. A recent study indicated that *Coccolithus pelagicus* and *E. huxleyi* possess voltage-gated H^+ channels, which are possibly involved in the removal of H^+ during calcification (Taylor et al. 2011). In this diploma thesis, no detailed measurements on the underlying processes of calcification were performed. Yet, the responses in PIC production are consistent with both explanations. Irrespective of the reasons, the lowered PIC production may have contributed to the boosted POC production, as both processes compete for C_i and energy (Rokitta & Rost subm.).

Chl *a* quota strongly increased under elevated pCO_2 (Fig. 3.3c) As pigmentation can be understood as a measure for “light harvesting capacity”, the higher chl *a* quota may reflect increased energy demand imposed by stimulated POC production. The chl *a*:POC ratio however, decreased with elevated pCO_2, indicating improved energy efficiency under ocean acidification (Fig. 3.4d). This phenomenon was also shown by Rokitta & Rost (subm.), who argued that the apparent energy surplus could be caused by a down regulation of the CCM activity under elevated pCO_2 (e.g. Kranz et al. 2009). However, Rokitta & Rost (subm.) did

not observe significant changes in C_i affinities or preferences in C_i sources in response to elevated pCO_2.

It is a common notion that CO_2 users are more sensitive to changes in CO_2 and consequently might benefit from ocean acidification to a larger extent (e.g. Rost et al. 2008). Although showing an exceptionally high sensitivity towards elevated pCO_2, *E. huxleyi* has been classified to be primarily a HCO_3^- user (Trimborn et al. 2007, Rokitta & Rost subm.). The ^{14}C disequilibrium technique, a widely applied method to determine carbon sources, is typically performed at standard pH, which in most cases does not reflect the pH under natural conditions. It is therefore fundamental to know whether the assay pH itself could impact the carbon uptake behavior of the examined species. For this reason, the instantaneous effects of the assay pH on the carbon uptake behavior of E. huxleyi were examined.

4.2 Bioassay

4.2.1 Carbon source assessment

By performing the ^{14}C disequilibrium technique over a range of ecologically relevant pH values, it could be demonstrated that the carbon uptake behavior of *E. huxleyi* (strain RCC 1216) was strongly dependent on the assay pH (Fig. 3.5). At low pH, cells preferentially used CO_2 for carbon uptake (pH 7.9 ≥90% CO_2 usage), whereas at high pH primarily HCO_3^- was taken up (pH 8.7 ~25% CO_2 usage). In contrast, the acclimation had no effect on the carbon uptake behavior. In other words, the f_{CO2} estimates were only dependent on the assay pH values.

Previous studies indicated that species regulate their C_i acquisition differently in response to pCO_2 acclimations (e.g. Rost et al. 2003; Trimborn et al. 2008, 2009). Measuring cellular C_i fluxes, Rost et al. (2003) found that the diatom *Skeletonema costatum*, for instance, is able to strongly regulate its CCM with changes in pCO_2. The haptophyte *Phaeocystis globosa*, however, neither modified its affinities nor preferences for C_i. Hence, there are species that regulate the mode of C_i acquisition in response to their acclimation history, while other species apparently constitutively express it.

The C_i acquisition of *E. huxleyi* (B92/11) was also found to be responsive to changes in pCO_2 (Rost et al. 2003). In contrast, measurements of photosynthetic O_2 evolution as a function of DIC could not detect any changes in C_i affinities in strain RCC 1216 (Rokitta & Rost, subm.). In the same study ^{14}C disequilibrium experiments were also carried out (at standard pH 8.5), yielding ~80% HCO_3^- usage in all treatments. In view of the finding of this diploma thesis, it can be expected that the constantly high HCO_3^- usage is an “artifact” of the conditions of the conventional assay.

Many other studies using the ^{14}C disequilibrium technique were performed at pH 8.5 (Elzenga et al. 2000, Tortell & Morel 2002; Martin & Tortell 2006; Tortell et al. 2008; Tortell

et al. 2010; Neven et al. 2010), which typically differed from the *in situ* pH values. In this diploma thesis, for instance, pH of the medium was ~8.2 and ~7.8 for low pCO_2 and high pCO_2, respectively (Fig. 4.1). For these values, the carbon uptake behavior was significantly different from that at pH 8.5. Cells grown at 380 μatm CO_2 show high CO_2 usage at pH 8.2 (~70 to 90 %) while cells grown at 950 μatm CO_2 likely express an even higher CO_2 usage of ≥90% when measured at the appropriate lower pH of 7.8. Thus, if measured only at one pH (that is possibly very different from the *in situ* pH values), the uptake behavior and also changes in C_i preferences due to pCO_2 treatments are masked.

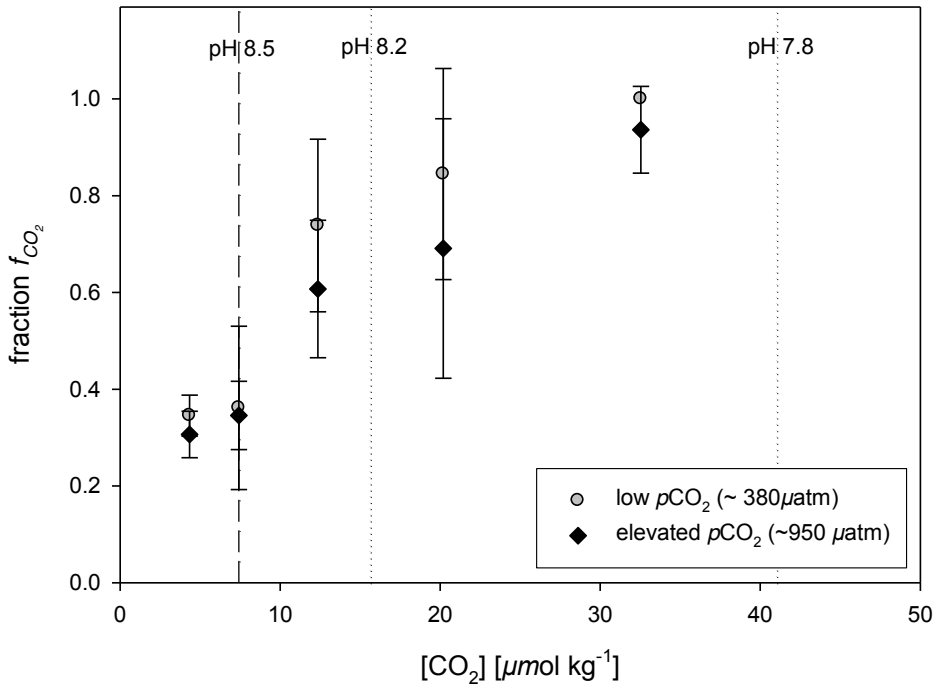

Fig. 4.1: Relative CO_2 usage f_{CO2} as a function of CO_2 concentrations in the assay media, acclimated to low pCO_2 (~380 μatm; grey circles) and elevated pCO_2 (~950 μatm; black diamonds). Slashed line indicates the pH value at which the assay is typically performed (pH 8.5); dotted lines indicate the *in situ* pH values of the acclimations in this study. Error bars indicate 1 SD, n ≥3. Corresponding statistical significance is presented in Table 3.2.

Tortell and co-workers (2008) intensively studied Southern Ocean phytoplankton, also applying the ^{14}C disequilibrium technique at pH 8.5. In most cases, a high HCO_3^- usage was observed (mean ~85%), irrespective of the *in situ* or the acclimation pH. Cassar et al. (2004) also applied the ^{14}C disequilibrium technique on Southern Ocean phytoplankton. Here, the assay was performed in unbuffered seawater at pH ~8.0, yielding an average HCO_3^- usage of ~50%. Although the compositions of the phytoplankton assemblages were certainly different between the two studies, the apparent offset in HCO_3^-/CO_2 usage is likely to originate from the different applied pH values during the assays. Approaches to assess carbon uptake behavior by means of MIMS are also typically performed at a stabilized pH (e.g. pH 8.0) and estimates may therefore also be biased by instantaneous pH. Rost et al. (2007) compared both, MIMS and ^{14}C disequilibrium technique, finding comparable f_{CO2} values. They concluded that

differences between approaches, including pH in the cell suspensions, do not affect the outcome. In view of the finding from this diploma thesis, data obtained by MIMS as well as ^{14}C disequilibrium technique may have to be re-evaluated.

Changes in the assay pH imply altered CO_2 concentrations in the medium (Table 3.1). The responses can therefore be attributed to CO_2 and/or pH. In Figure 4.1, the results on f_{CO2} estimates are expressed as a function of the CO_2 concentration in the assay medium. The increasing CO_2 usage with increasing CO_2 concentration may be attributed to enhanced diffusive CO_2 supply, improved CO_2 availability for CO_2 transporters and/or decreased CO_2 leakage. As a consequence, higher internal CO_2 concentration could enhance the $[CO_2]$:$[O_2]$ ratio in the proximity of RubisCO. Resulting changes in level of photorespiration metabolites may trigger the regulation of CCMs (Kaplan et al. 2001), for instance the activity of HCO_3^- transporters.

As an increase of external H^+ concentration results also in an intracellular rise of H^+ levels (Suffrian et al. 2011), ocean acidification might as well shift the speciation of intracellular DIC toward higher CO_2 concentrations. H^+ concentration could also directly affect the activity of enzymes by protonation-controlled changes in conformation or it may influences the energization of C_i transporters by altering the electrochemical membrane potential (Suffrian et al. 2011). To distinguish between effects of H^+ and CO_2, it might be useful to modify the assay in such a way that pH is kept constant, while CO_2 concentrations are varied (Bach et al. 2011; Langer & Bode 2011).

4.2.2 Sensitivity study

The outcome of the ^{14}C disequilibrium technique is based on fit functions, for which certain parameters ($\alpha1$, $\alpha2$, $\Delta SA_{HCO3-}/SA_{DIC}$, $\Delta SA_{CO2}/SA_{DIC}$) have to be adjusted to the specific conditions (e.g. T or pH). An underlying assumption is that those remain constant. However, pH of buffers may drift over time, and even if calibrated carefully, pH electrodes are often imprecise. To strengthen the results, pH values of buffered media and spike were re-measured prior to the assay and the fitting procedure was repeated with the adjusted parameters (Table 3.1). This procedure improved the significance of differences between treatments, but did not change the overall outcome (Table 3.2). Since also other parameters in the experimental setup might be biased, a sensitivity study was performed to estimate whether and to which extent offsets in pH and T may influence the outcome of the assay.

Model runs were performed using idealized ^{14}C incorporation curves with "correct" and "biased" parameter settings (T ±2°C; pH ±0.05). Resulting correct and biased f_{CO2} values were compared. Erroneous pH or T values mainly affected the f_{CO2} estimates of CO_2 users (Fig. 3.7). Offsets in estimated f_{CO2} values were up to 20 percentage points, but these errors would not mask the overall pH-dependent carbon uptake behavior because the detected differences in f_{CO2} were greater than 60 percentage points over the tested pH range (Fig 3.5).

Much more pronounced offsets in f_{CO2} estimates were caused by erroneous blank values, a phenomenon that, again, mainly applies to CO_2 users (Fig. 3.8). For final ^{14}C fixation rates of ≤4 dpm s^{-1}, a blank offset by 100 dpm changed the resulting f_{CO2} by up to 50 percentage points. In this diploma thesis, final ^{14}C fixation rates were between 0.5 and 5 dpm s^{-1} and thus very sensitive to errors in blank estimations. Elevating the biomass in the assay or using a higher ^{14}C activity reduces the potential errors in f_{CO2} estimates. Higher cell densities may, however, introduce detrimental effects such as self shading or the buildup of high O_2 levels. Increasing specific activities may ultimately induce not only an isotopic but also a chemical disequilibrium, again causing a different carbon uptake behavior. In view of these limitations, more effort should be put into careful degassing of samples and taking multiple blank measurements.

The CO_2 users in this sensitivity study showed a generally higher sensitivity towards erroneous parameter settings, because small changes in the carbon uptake behavior translate into stronger changes in the curvature of the ^{14}C incorporation curve and ultimately f_{CO2} estimates. This can also explain why in this diploma thesis, the uncertainty of f_{CO2} estimates were largest at low pH values, where cells preferentially used CO_2 as carbon source (Fig. 3.5, 4.1). At the lowest pH, this effect was less “visible” because the model is restricted to f_{CO2} values ≤1. The sensitivity study indicates that the ^{14}C disequilibrium technique is a very robust assay that delivers reliable results, even if fitting parameters are largely biased as tested here. This makes it a straightforward method that is useful for resolving the carbon uptake behavior of a variety of species, especially in shipboard or field studies.

4.2.3 Carbon fixation rates

Under both acclimations, C_i fixation rates obtained from the final slope of ^{14}C incorporation varied between ~30 to 200 μmol C (mg chl *a*)$^{-1}$ h^{-1} (Fig. 3.9). In *E. huxleyi*, measurements of O_2 evolution yielded rates of ~150 to 650 µmol O_2 (*m*g chl *a*)$^{-1}$ h^{-1} (Nielsen et al. 1995; Rost et al. 2003; Houdan et al. 2005). These rates are comparable when accounting for a photosynthetic quotient of 1.4 (in NO_3-grown cells; Williams & Robertson 1991) and the fact that rates of O_2 evolution were determined under higher light intensities. Rates of C_i fixation strongly fluctuated. This large variability could be caused by small differences in temperature or light intensities between assay runs, the latter most likely being below saturation. Also, diurnal changes (Zondervan et al. 2002, Van Bleijswijk et al. 1994) and/or erroneous chl *a* normalization may have contributed to the high variability. For this reason, these short-term C fixation rates cannot be used to explain the increasing POC production under elevated pCO_2 in the acclimations. In principle, however, if more accurate rates of C fixation were obtained, they could be used in combination with the f_{CO2} estimates to derive CO_2 and HCO_3^- uptake rates for the respective conditions.

4.3 Biogeochemical implications

The presented results indicate that *E. huxleyi* RCC 1216 is highly sensitive to changes in carbonate chemistry, both in terms of acclimation responses (e.g. PIC/POC production) as well as the underlying processes (i.e. C_i uptake behavior). The apparent increase in CO_2 usage under low pH / high CO_2 concentration could explain the higher POC production under elevated pCO_2. In contrast to previous studies, in this diploma thesis, *E. huxleyi* was classified as a CO_2 user even under 380 μatm CO_2.

In view of the lowered rates/degrees of calcification, although its function remains unknown, it can be suspected that coccolithophores like *E. huxleyi* will suffer from ocean acidification (e.g. Riebesell et al. 2000; Zondervan et al. 2001; Rost and Riebesell 2004; Langer et al. 2009). Even within the group of coccolithophores, ocean acidification may cause a shift from more heavily to less calcified species or strains, indicating that the degree of calcification represents a selective trait (Beaufort et al. 2011). Consequently, coccolithophores may be outcompeted by non-calcifying phytoplankton in the future ocean.

Regarding the increase in biomass production as well as POC:PON ratio under ocean acidification, however, there are indications for improved resource management. The higher relative usage of CO_2, as indicated from the ^{14}C disequilibrium assays, may significantly reduce the costs of the CCM and hence increase the energy availability for the cell. In addition, the higher POC:PON ratio implies an optimized nutrient use efficiency (Reinfelder 2011). Thus, the observed alterations in biomass production suggest that *E. huxleyi* might even benefit from ocean acidification.

An altered PIC:POC ratio, caused by changes in cellular rates but also by shifts in species composition, implies that also the relative strengths of the biological carbon pumps are affected (Rost & Riebesell 2004). The organic carbon pump may become stronger due to increased POC production. Concomitantly, the carbonate counter pump may weaken due to reduced calcification. Both processes imply a higher CO_2 uptake capacity of the ocean. Since the ballast-driven transfer of biomass might be less efficient, however, predicting the overall effect of altered PIC:POC ratios on the CO_2 gas exchange between oceans and atmosphere remains challenging.

References

Armstrong, R.A., C. Lee, J.I. Hedges, S. Honjo, and S.G. Wakeham. 2002. A new, mechanistic model for organic carbon fluxes in the ocean based on the quantitative association of POC with ballast minerals. *Deep-Sea Res Pt II*. 49:219 - 236.

Asada, K. 1999. The water-water cycle in chloroplasts: scavenging of active oxygens and dissipation of excess photons. *Annu Rev Plant Physiol Plant Mol Biol*. 50:601–639.

Badger, M.R., A. Kaplan, J.A., Berry. 1977. The internal CO_2 pool of *Chlamydomonas reinhardtii*: Response to external CO_2. Carnegie Institute Year Book 76:362–366.

Badger, M.R., A. Kaplan, and J.A. Berry. 1980. Internal inorganic carbon pool of *Chlamydomonas reinhardtii*. Evidence for a CO_2 concentrating mechanism. *Plant Physiol*. 66:407–413.

Badger, M.R., K. Palmqvist, and J.W. Yu. 1994. Measurement of CO_2 and HCO_3^- fluxes in cyanobacteria and microalgae during steady-state photosynthesis. *Plant Physiol*. 90:529.

Badger, M.R., T.J. Andrews, S.M. Whitney, M. Ludwig, and D.C. Yellowlees. 1998. The diversity and co-evolution of Rubisco, plastids, pyrenoids and chloroplast-based CO_2-concentrating mechanisms in the algae. *Can J Bot*. 76:1052.

Beaufort, L., I. Probert, T. de Garidel-Thoron, E.M. Bendif, D. Ruiz-Pino, N. Metzl, C. Goyet, N. Buchet, P. Coupel, M. Grelaud, B. Rost, R.E.M. Rickaby, and C. de Vargas. 2011. Sensitivity of coccolithophores to carbonate chemistry and ocean acidification. *Nature*. 476:80-83.

Berry, J.A., J. Boynton, A. Kaplan, and M.R. Badger. 1976. Growth and photosynthesis of Chlamydomonas reinhardtii as a function of CO2 concentration. *Carnegie Institute Wash Year Book* 75:423–432.

Berry, L., A.R. Taylor, U. Lucken, K.P. Ryan, and C. Brownlee. 2002. Calcification and inorganic carbon acquisition in coccolithophores. *Funct Plant Biol* 29:289-299.

Dickson, A.G. 1981. An Exact Definition of Total Alkalinity and a Procedure for the Estimation of Alkalinity and Total Inorganic Carbon from Titration Data. *Deep-Sea Res Pt II*. 28:609-623.

Dickson, A.G., and F.J. Millero. 1987. A comparison of the equilibrium constants for the dissociation of carbonic acid in seawater media. *Deep-Sea Res Pt I*. 34:1733-1743.

Elzenga, J.T.M., H.B.A. Prins, and J. Stefels. 2000. The role of extracellular carbonic anhydrase activity in inorganic carbon utilization of *Phaeocystis globosa* (Prymnesiophyceae): a comparison with other marine algae using the isotopic disequilibrium technique. *Limnol Oceanogr*. 45:372.

Engel, A., I. Zondervan, K. Aerts, L. Beaufort, A. Benthien, L. Chou, B. Delille, J.P. Gattuso, J. Harlay, C. Heemann, L. Hoffmann, S. Jacquet, J. Nejstgaard, M.D. Pizay, E. Rochelle-Newall, U. Schneider, A. Terbrueggen, and U. Riebesell. 2005. Testing the direct effect of CO2 concentration on a bloom of the coccolithophorid *Emiliania huxleyi* in mesocosm experiments. *Limnol Oceanogr*. 50:493-507.

Espie, G.S., and B. Colman. 1986. Inorganic Carbon Uptake during Photosynthesis - A Theoretical Analysis Using the Isotopic Disequilibrium Technique. *Plant Physiol*. 80:863-869.

Falkowski, P.G. 1997. Evolution of the nitrogen cycle and its influence on the biological sequestration of CO_2 in the ocean. *Nature*. 387:272-275.

Falkowski, P.G., R.T. Barber, and V. Smetacek. 1998. Biogeochemical Controls and Feedbacks on Ocean Primary Production. *Science*. 281:200-206.

Falkowski, P., R.J. Scholes, E. Boyle, J. Canadell, D. Canfield, J. Elser, N. Gruber, K. Hibbard, P. Hogberg, S. Linder, F.T. Mackenzie, B.I. Moore, T. Pedersen, Y. Rosenthal, S. Seitzinger, V. Smetacek, and W. Steffen. 2000. The Global Carbon Cycle: A Test of Our Knowledge of Earth as a System. *Science*. 290:291-296.

Good, E., G.D. Winget, W. Winter, T.M. Connolly, S. Izawa, and R.M.M. Sing. 1966. Hydrogen Ion Buffers for Biological Research. *Biogeochemistry*. 5.

Graham, D., and C.P. Whittingham. 1968. The path of carbon during photosynthesis in Chlorella pyrenoidosa at high and low carbon dioxide concentrations. *Z Pflanzenphysiol*.

Guillard, R.R.L., and J.H. Ryther. 1962. Studies of marine planktonic diatoms. *Can J Microbiol*. 8:229-239.

Herfort, L., E. Loste, F. Meldrum, and B. Thake. 2004. Structural and physiological effects of calcium and magnesium in *Emiliania huxleyi* (Lohmann) Hay and Mohler. *J Struct Biol*. 148:307-314.

Holligan, P.M., E. Fernandez, J. Aiken, W.M. Balch, P. Boyd, P.H. Burkill, M. Finch, S.B. Groom, G. Malin, K. Muller, D.A. Purdie, C. Robinson, C.C. Trees, S.M. Turner, and P. Vanderwal. 1993. A biogeochemical study of the coccolithophore, *Emiliania huxleyi,* in the North-Atlantic. *Global Biogeochem Cy*. 7:879-900.

Holm-Hansen, O., and B. Riemann. 1978. Chlorophyll a determination: improvements in methodology. *Oikos*. 30:438-447.

Hoppe, C.J.M., G. Langer, and B. Rost. 2011. *Emiliania huxleyi* shows identical responses to elevated pCO_2 in TA and DIC manipulations. *JEMBE*. 406:54-62.

Johnson, K.S. 1982. Carbon dioxide hydration and dehydration kinetics in seawater. *Limnol. Oceanogr.* 27:849.

Kaplan, A., M.R. Badger, and J.A. Berry. 1980. Photosynthesis and the intracellular inorganic carbon pool in the blue green alga *Anabaena variabilis*: Response to external CO_2 concentration. *Planta*. 149:219-226.

Kaplan, A., Y. Helman, D. Tchernov, and L. Reinhold. 2001. Acclimation of photosynthetic microorganisms to changing ambient CO_2 concentration. *P Natl Acad Sci USA*. 98:4817-4818.

Kranz, S.A., D. Sueltemeyer, K.-U. Richter, and B. Rost. 2009. Carbon acquisition in *Trichodesmium*: the effect of pCO_2 and diurnal changes. *Limnol Oceanogr*. 54:548-559.

Kranz, S.A., O. Levitan, K.-U. Richter, O. Prasil, I. Berman-Frank, and B. Rost. 2010. Combined Effects of CO_2 and Light on the N_2-Fixing Cyanobacterium *Trichodesmium* IMS101: Physiological Responses. *Plant Physiol*. 154:334-345.

Langer, G., N. Gussone, G. Nehrke, U. Riebesell, A. Eisenhauer, H. Kuhnert, B. Rost, S. Trimborn, and S. Thoms. 2006. Coccolith strontium to calcium ratios in *Emiliania huxleyi*: The dependence on seawater strontium and calcium concentrations. *Limnol Oceanogr* 51:310–320.

Langer, G., G. Nehrke, I. Probert, J. Ly, and P. Ziveri. 2009. Strain-specific responses of *Emiliania huxleyi* to changing seawater carbonate chemistry. *Biogeosciences*. 6:2637-2646.

Langer, G., and M. Bode. 2011. CO_2 mediation of adverse effects of seawater acidification in *Calcidiscus leptoporus*. *Geochemistry Geophysics Geosystems*. 12.

Leonardos, N., and R.J. Geider. 2005. Elevated atmospheric carbon dioxide increases organic carbon fixation by *Emiliania huxleyi* (Haptophyta), under nutrient-limited high-light conditions. *J Phycol*. 41:1196-1203.

Lüthi, D., M. Le Floch, B. Bereiter, T. Blunier, J.M. Barnola, U. Siegenthaler, D. Raynaud, J. Jouzel, H. Fischer, K. Kawamura, and T.F. Stocker. 2008. High-resolution carbon dioxide concentration record 650,000-800,000 years before present. *Nature*. 453:379-382.

Martin, C.L., and P.D. Tortell. 2006. Bicarbonate transport and extracellular carbonate anhydrase in Bering Sea phytoplankton assemblages: Results from isotopic disequilibrium experiments. *Limnol Oceanogr* 51:2111–2121.

Mehrbach, C., C.H. Culberson, J.E. Hawley, and R.M. Pytkowicz. 1973. Measurement of the Apparent Dissociation Constants of Carbonic Acid in Seawater at Atmospheric Pressure. *Limnol Oceanogr* 18:897-907.

Merico, A., T. Tyrrell, C.W. Brown, S.B. Groom, and P.I. Miller. 2003. Analysis of satellite imagery for Emiliania huxleyi blooms in the Bering Sea before 1997. *Geophys Res Lett*. 30.

Millero, F.J., and R.N. Roy. 1997. A chemical equilibrium model for the carbonate system in natural waters. *Croatica Chemica Acta*. 70:1-38.

Neven, I.A., J. Stefels, S. van Heuven, H.J.W. de Bar, and J.T.M. Elzenga. 2011. High plasticity in inorganic carbon uptake by Southern Ocean phytoplankton in response to ambient CO_2. *Deep-Sea Res PT II*

Nielsen, M.V. 1995. Photosynthetic Characteristics of The Coccolithophorid Emiliania-huxleyi (Prymnesiophyceae) exposed to elevated concentrations of dissolved inorganic carbon. *J Phycol*. 31:715-719.

Pacala, S.W., G.C. Hurtt, D. Baker, P. Peylin, R.A. Houghton, R.A. Birdsey, L. Heath, E.T. Sundquist, R.F. Stallard, P. Ciais, P. Moorcroft, J.P. Caspersen, E. Shevliakova, B. Moore, G. Kohlmaier, E. Holland, M. Gloor, M.E. Harmon, S.M. Fan, J.L. Sarmiento, C.L. Goodale, D. Schimel, and C.B. Field. 2001. Consistent land- and atmosphere-based US carbon sink estimates. *Science*. 292:2316-2320.

Paasche, E. 1964. A tracer study of the inorganic carbon uptake during coccolith formation and photosynthesis in the coccolithophorid *Coccolithus huxleyi*. *Scandinavian Society for Plant Physiology.*

Pearson, P.N., and M.R. Palmer. 2000. Atmospheric carbon dioxide concentrations over the past 60 million years. *Nature*. 406:695-699.

Petit, J.R., J. Jouzel, D. Raynaud, N.I. Barkov, J.M. Barnola, I. Basile, M. Bender, J. Chappellaz, M. Davis, G. Delaygue, M. Delmotte, V.M. Kotlyakov, M. Legrand, V.Y. Lipenkov, C. Lorius, L. Pepin, C. Ritz, E. Saltzman, and M. Stievenard. 1999. Climate and atmospheric history of the past 420,000 years from the Vostok ice core, Antarctica. *Nature*. 399:429-436.

Pierrot, N., S.F. Santos, C. Feyt, M. Morel, J.P. Brion, and J.N. Octave. 2006. Calcium-mediated transient phosphorylation of tau and amyloid precursor protein followed by intraneuronal amyloid-beta accumulation. *JBiol Chem*. 281:39907-39914.

Raghavendra, A.S., and K. Padmasree. 2003. Beneficial interactions of mitochondrial metabolism with photosynthetic carbon assimilation. *Trends Plant Sci*. 8:546-553.

Raupach, M.R., G. Marland, P. Ciais, C. Le Quere, J.G. Canadell, G. Klepper, and C.B. Field. 2007. Global and regional drivers of accelerating CO_2 emissions. *PNAS*. 104:10288-10293.

Raven, J.A., and A.M. Johnston. 1991. Mechanisms of inorganic-carbon acquisition in marine-phytoplankton and their implications for the use of other resources. *Limnol Oceanogr*. 36:1701-1714.

Raven, J.A. 1997. CO_2 concentrating mechanisms: a role for thylakoid lumen acidification. *Plant Cell Environ*. 20:147.

Reinfelder, J.R., A.M.L. Kraepiel, and F.M.M. Morel. 2000. Unicellular C4 photosynthesis in a marine diatom. *Nature*. 407:996.

Reinfelder, J.R., A.J. Milligan, and F.M.M. Morel. 2004. The role of C4 photosynthesis in carbon accumulation and fixation in a marine diatom. *Plant Physiol*. 135:2106.

Reinfelder, J.R. 2011. Carbon Concentrating Mechanisms in Eukaryotic Marine Phytoplankton. *Ann Rev Mar Sci*. 3:291-315.

Richier, S., S. Fiorini, M.-E. Kerros, P. Von Dassow, and J.-P. Gattuso. 2011. Response of the calcifying coccolithophore *Emiliania huxleyi* to low pH/high pCO_2: from physiology to molecular level. *Mar. Biol.* 158:551-560.

Riebesell, U., S. Burkhardt, M. Pahlow, A. Wischmeyer, and D. Wolf-Gladrow. 1997. Algal responses to increasing CO_2 concentrations. *Phycologia*. 36:93-93.

Riebesell, U., I. Zondervan, B. Rost, P.D. Tortell, E. Zeebe, and F.M.M. Morel. 2000. Reduced calcification in marine plankton in response to increased atmospheric CO_2. *Nature*. 407:634-637.

Roberts, K., E. Granum, R.C. Leegood, and J.A. Raven. 2007. C-3 and C-4 pathways of photosynthetic carbon assimilation in marine diatoms are under genetic, not environmental, control. *Plant Physiol.* 145:230-235.

Rokitta, S.D., L.J. De Nooijer, S. Trimborn, C. De Vargas, B. Rost, and U. John. 2011. Transcriptome analyses reveal differential gene expression patterns between life-cycle stages of *Emiliania huxleyi* (Haptophyta) and reflect specialization to different ecological niches. *J. Phycol*. 47:829-838.

Rokitta, S.D., and B. Rost. subm. Effects of pCO_2 and their modulation by light in the life-cycle stages of the coccolithophore *Emiliania huxleyi*. *Limnol Oceanogr*.

Rost, B., I. Zondervan, and U. Riebesell. 2002. Light-dependent carbon isotope fractionation in the coccolithophorid *Emiliania huxleyi*. *Limnol Oceanogr*. 47:120-128.

Rost, B., U. Riebesell, S. Burkhardt, and D. Sueltemeyer. 2003. Carbon acquisition of bloom-forming marine phytoplankton. *Limnol Oceanogr*. 48:55.

Rost, B., and U. Riebesell. 2004. Coccolithophores and the biological pump: responses to environmental changes. *In* Coccolithophores—From Molecular Processes to Global Impact. H.R. Thierstein and E.B. Young, editors. Springer. 76–99.

Rost, B., I. Zondervan, and D. Wolf-Gladrow. 2008. Sensitivity of phytoplankton to future changes in ocean carbonate chemistry: Current knowledge, contradictions and research directions. *Mar ecol-prog ser*. 373:227-237.

Sarmiento, J.L., M. R., and L.Q. C. 1995. Air-sea CO_2 transfer and the carbon budget of the North Atlantic. *Philos T Roy Soc B*. 348:211-219.

Sarmiento, J.L., R. Slater, R. Barber, L. Bopp, S.C. Doney, A.C. Hirst, J. Kleypas, R. Matear, U. Mikolajewicz, P. Monfray, V. Soldatov, S.A. Spall, and R. Stouffer. 2004. Response of ocean ecosystems to climate warming. *Global Biogeochem Cy*. 18.

Schulz, K.G., B. Rost, S. Burkhardt, U. Riebesell, S. Thoms, and D.A. Wolf-Gladrow. 2007. The effect of iron availability on the regulation of inorganic carbon acquisition in the coccolithophore *Emiliania huxleyi* and the significance of cellular compartmentation for stable carbon isotope fractionation. *Geochim. Cosmochim. Acta*. 71:5301-5312.

Sikes, C.S., and K.M. Wilbur. 1980. Calcification by coccolithophorids - effects of pH AND SR. *J Phycol*. 16:433-436.

Solomon, S., M. Qin, Z. Manning, M. Chen, Marquis, K.B. Averyt, M. Tignor, and H.L. Miller. 2007. Climate Change 2007: The Physical Science Basis. Contribution of Working Group I to the Fourth Assessment Report of the Intergovernmental Panel on Climate Change. Cambridge University Press, Cambridge, United Kingdom and New York, NY, USA.

Stoll, M.H.C., K. Bakker, G.H. Nobbe, and R.R. Haese. 2001. Continuous-Flow Analysis of Dissolved Inorganic Carbon Content in Seawater. *Anal Chem*. 73:4111-4116.

Stumm, W., and J.J. Morgan. 1996. Aquatic Chemistry, Wiley & Sons, New York.

Suffrian, K., K.G. Schulz, M.A. Gutowska, U. Riebesell, and M. Bleich. 2011. Cellular pH measurements in *Emiliania huxleyi* reveal pronounced membrane proton permeability. *New Phytol*. 190:595-608.

Sültemeyer, D., G. Amoroso, and H.P. Fock. 1995. Induction of intracellular carbonic anhydrases during the adaptation to low inorganic carbon concentrations in wild-type and ca-1 mutant cells of *Chlamydomonas reinhardtii*. *Planta*. 196:217.

Taylor, A.R., and C. Brownlee. 2005. Unravelling the Mechanisms of Calcium Transport in Coccolithophores. *Phycologia*. 44:14-15.

Taylor, A.R., A. Chrachi, G. Wheeler, H. Goddard, and C. Brownlee. 2011. A Voltage-Gated H^+ Channel Underlying pH Homeostasis in Calcifying Coccolithophores. *PLoS Biol* 9:14pp.

Tortell, P.D., and F.M.M. Morel. 2002. Sources of inorganic carbon for phytoplankton in the eastern Subtropical and Equatorial Pacific Ocean. *Limnol Oceanogr*. 47:1012–1022.

Tortell, P.D., C.L. Martin, and M.E. Corkum. 2006. Inorganic carbon uptake and intracellular assimilation by subarctic Pacific phytoplankton assemblages. *Limnol Oceanogr*. 51:2102-2110.

Tortell, P.D., C.D. Payne, Y. Li, S. Trimborn, B. Rost, W.O. Smith, C. Riesselman, R. Dunbar, P. Sedwick, and G. DiTullio. 2008. The CO_2 response of Southern Ocean phytoplankton. *Geophys Res Lett*. 35:L04605.

Tortell, P.D., S. Trimborn, Y.Y. Li, B. Rost, and C.D. Payne. 2010. Inorganic Carbon Utilization by Ross Sea Phytoplankton Across Natural and Experimental CO_2 Gradients. *J Phycol*. 46:433-443.Trimborn, S., G.

Trimborn, S., N. Lundholm, S.A. Thoms, K.-U. Richter, B. Krock, P.J. Hansen, and B. Rost. 2008. Inorganic carbon acquisition in potentially toxic and non-toxic diatoms: the effect of pH-induced changes in seawater carbonate chemistry. *Physiol Plantarum*. 133:92-105.

Trimborn, S., D. Wolf-Gladrow, K.-U. Richter, and B. Rost. 2009. The effect of pCO_2 on carbon acquisition and intracellular assimilation in four marine diatom species. *Journal of Experimental Marine Biology and Ecology*. 376:26-36.

Vogel, J.C., P.M. Grootes, and W.G. Mook. 1970. Isotopic Fractionation Between Geaseous and Dissolved Carbon Dioxide *Zeitschrift Fur Physik*. 230:225.

Von Dassow, P., H. Ogata, I. Probert, P. Wincker, C. Da Silva, S. Audic, J.-M. Claverie, and C. De Vargas. 2009. Transcriptome analysis of functional differentiation between haploid and diploid cells of *Emiliania huxleyi*, a globally significant photosynthetic calcifying cell. *Genome Biol.* 10.

Weiss, R.F. 1974. Carbon dioxide in water and seawater: The solubility of a non-ideal gas. *Mar Chem*. 2:203-215.

Westbroek, P., C.W. Brown, J. Vanbleijswijk, C. Brownlee, G.J. Brummer, M. Conte, J. Egge, E. Fernandez, R. Jordan, M. Knappertsbusch, J. Stefels, M. Veldhuis, P. Vanderwal, and J. Young. 1993. A Model system approach to biological climate forcing - the example of *Emiliania-Huxleyi*. *Global Planet Change*. 8:27-46.

Wolf-Gladrow, D.A., R.E. Zeebe, C. Klaas, A. Koertzinger, and A.G. Dickson. 2007. Total alkalinity: The explicit conservative expression and its application to biogeochemical processes. *Mar Chem*. 106:287-300.

Zeebe, R.E., and D.A. Wolf-Gladrow. 2007. CO_2 in seawater: equilibrium, kinetics, isotopes. Elsevier Science B.V., Amsterdam.

Zondervan, I., R.E. Zeebe, B. Rost, and U. Riebesell. 2001. Decreasing marine biogenic calcification: A negative feedback on rising atmospheric pCO_2. *Global Biogeochemical Cycles*. 15:507-516.

Zondervan, I., B. Rost, and U. Riebesell. 2002. Effect of CO_2 concentration on the PIC/POC ratio in the coccolithophore *Emiliania huxleyi* grown under light-limiting conditions and different daylengths. *JEMBE*. 272:55-70.

Zondervan, I. 2007. The effects of light, macronutrients, trace metals and CO_2 on the production of calcium carbonate and organic carbon in coccolithophores - A review. *Deep-Sea Res Pt II*. 54:521-537.